MQP KZS-RMPF

Markhor: Robotic Mining Platform

A Major Qualifying Project

Submitted to the Faculty of

Worcester Polytechnic Institute

in partial fulfillment of the requires for the

Degree in Bachelor of Science

in

Robotics Engineering

Mechanical Engineering

and Computer Science

SUBMITTED BY:

Domenic Bozzuto, Robotic Engineering and Computer Science

Rene Jacques, Robotic Engineering

Aaron Jaeger, Robotic Engineering

Brian Peterson, Mechanical Engineering

Yu-sen Wu, Robotic Engineering and Mechanical Engineering

ADVISED BY:

Kenneth Stafford, Robotic Engineering and Mechanical Engineering

Michael Ciaraldi, Robotic Engineering and Computer Science

Abstract

In-situ resource utilization, or the use of the resources available in a foreign environment, is crucial to the success of manned missions to Mars; however, it is a severely underdeveloped technology. This project explores the development of a rover capable of operating in a simulated Martian environment. The rover is capable of mining large amounts of simulated ice chunks from below the surface, driving its payload to a collection station, and unloading all of the collected material. This project is partially inspired by NASA's Robotic Mining Competition which served to establish a set of guidelines around which the robot was constructed.

Acknowledgements

We would like to thank our advisors Michael Ciaraldi and Kenneth Stafford for their constant input and advice over the duration of this project. We would also like to thank Toby Bergstrom for the use of his office, James Loiselle for assisting us with manufacturing, and Michael Gennert for providing construction material. We would also like to thank those that sponsored this project: BRECOflex, Hydro-Cutter, Worcester Sand and Gravel, and the Robotics, Mechanical, and Computer Science Departments at WPI.

Contents

List of Figures

1 Background

Since the early 60s, an incredible amount of research and development has been devoted to learning more about Mars, the fourth planet in our solar system. In the past two decades, this research has evolved from simply observing Mars through a telescope to actually landing rovers on the surface of Mars, which collect and transmit data over 54 million kilometers back to Earth. While the means of researching the planet have changed drastically since the 60s, one of the core goals has not changed: determining whether Mars was ever capable of supporting life, and whether it could support life in the future. This is typically done by analyzing samples of minerals on the planet's surface via rovers. The rovers that have been sent to Mars in the past have been mobile laboratories capable of digging 5 cm deep for sample collection and analysis. The discovery of water and carbon dioxide (CO_2) motivates the development of a rover capable of digging to significantly deeper depths and collecting material for resource utilization. To encourage the development of this type of rover, the National Aeronautics and Space Administration (NASA) conducts the Robotics Mining Challenge (RMC) annually, where undergraduates design robotic excavation platforms. The goal of this project is to develop a rover that is capable of collecting materials over 30 cm below the surface and returning them to a collection site. In order to better understand the scenario, research was done on the following topics:

- previous Missions to Mars,
- the Martian environment,
- the NASA Robotics Mining Competition, and
- existing solutions to resource collection

1.1 Missions to Mars

Since 1997, NASA has sent four rovers to Mars to collect data about the planet. These rovers are Sojourner, Spirit, Opportunity, and Curiosity. As technology continued to develop, the complexity and capabilities of these rovers greatly increased.

1.1.1 Sojourner

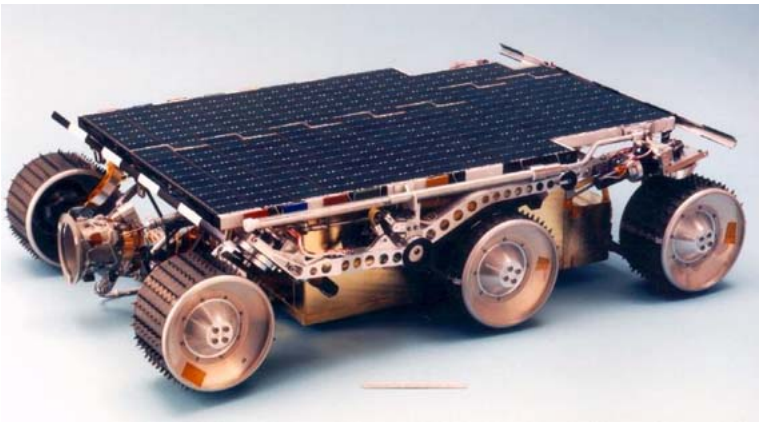

Figure 1: Sojourner rover

[1] The first rover sent to Mars was Sojourner, shown in Figure 1, which was part of the Pathfinder mission. This rover landed on Mars on July 4th, 1997; for the following 85 days, it collected and transmitted data back to NASA headquarters on Earth.[2] Data collected from Sojourner included over 500 pictures taken by the rover, 15 chemical analyses of soil and rocks, and additional information on wind speeds and weather. Sojourner used a six-wheel rocker-bogie system to allow it to traverse over obstacles up to 13 cm tall, and has a top speed of 0.40 m/minute.[3] The rover also used an on-board camera to avoid obstacles and to generate a panoramic photo at the end of each day of the mission. Sojourner was relatively simple compared to the other robots that would later be deployed to Mars; however, information gained from the Pathfinder mission nonetheless proved to be very insightful in the development and deployment of future rovers.

1.1.2 Spirit and Opportunity

The next machines to be deployed to Mars were an identical pair of rovers known as Spirit and Opportunity - a rendering of Spirit is shown in Figure 2. These robots arrived on Mars on January 3rd, 2003 and January 24th, 2003, respectively.[4] Spirit and Opportunity were both deployed in order to search for evidence of water on Mars, which was achieved by taking images of their surroundings and analyzing rock samples. The information collected from the rovers indicated that water used to exist in several locations including the Gusev Crater, Colombia Hills, and the

[1] https://mars.jpl.nasa.gov/MPF/rover/sim2.jpg
[2] http://www.nasa.gov/mission_pages/mars-pathfinder/
[3] http://mars.jpl.nasa.gov/MPF/rover/descrip.html
[4] http://mars.nasa.gov/programmissions/missions/present/2003/

Victoria Crater.

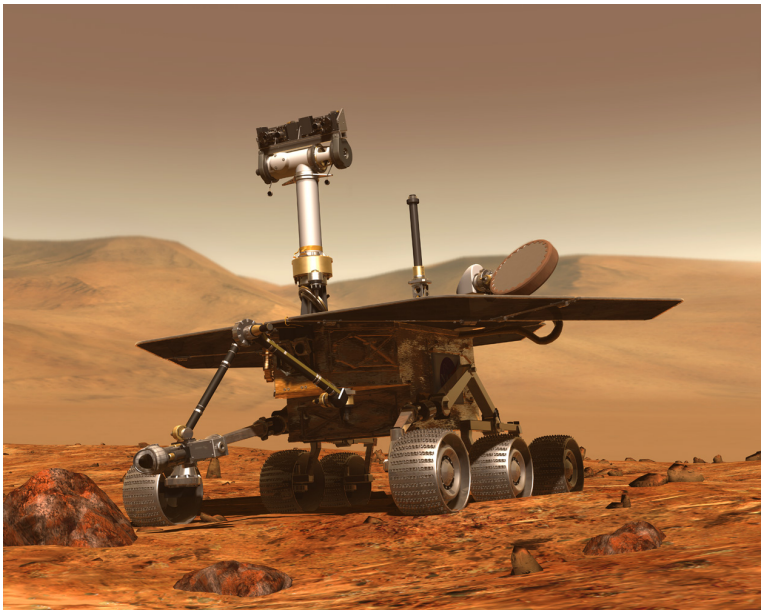

Figure 2: Rendering of the Spirit rover

[5]

Similar to Sojourner, both of these rovers operated with a six-wheel rocker-bogie drivetrain. Spirit and Opportunity, however, included many more tools and accessories to provide a more-detailed analysis of the environment, including a thermal emission spectrometer, an alpha particle x-ray spectrometer, and a microscopic imager.[6] These tools were all used to analyze rocks and minerals on the surface of the planet. In May 2009, Spirit entered an unexpected sand trap that prevented it from moving any further.[7] Prior to this occurrence, one of Spirit's wheels had failed and no longer functioned, which scientists at NASA believe was a result of the electronic motor controller failing. This failure combined with the low cohesion properties of the soil prevented the rover from ever escaping the hole. Opportunity, on the other hand, continues to transmit data back to Earth.

[5]https://en.wikipedia.org/wiki/Spirit_(rover)
[6]http://mars.nasa.gov/mer/newsroom/factsheets/pdfs/Mars03Rover041020.pdf
[7]http://news.bbc.co.uk/2/hi/8481798.stm

1.1.3 Curiosity

Figure 3: Curiosity rover

[8] The most recent rover to be deployed on Mars is Curiosity (shown in Figure 3), which was launched in November, 2011, and arrived on the surface of Mars in August of the following year.[9] The primary mission for Curiosity evolved from looking for signs of water to searching for signs that prove Mars was once capable of supporting life. To accomplish this goal, Curiosity analyzes the chemical compositions of soil samples and looks for the presence of certain elements (like carbon) that are necessary for sustaining life. Since its arrival, the rover has analyzed countless rock samples. Curiosity uses a drill to extract samples in combination with its ChemCam laser vaporization system which measures the composition of vaporized materials. These material evaporations have shown the presence of complex organic molecules, which strongly hint at the previous existence of some form of life.

1.2 Environment

The Martian environment presents an overwhelming list of challenges that a rover must face; these challenges stem from the topography, atmospheric conditions, and subterranean characteristics of the planet. This harsh environment dictates which systems will not function properly on Mars and are crucial to consider in the design of a Martian rover.

[8] http://photo.sf.co.ua/g/233/1.jpg
[9] http://www.space.com/17963-mars-curiosity.html

1.2.1 Topography

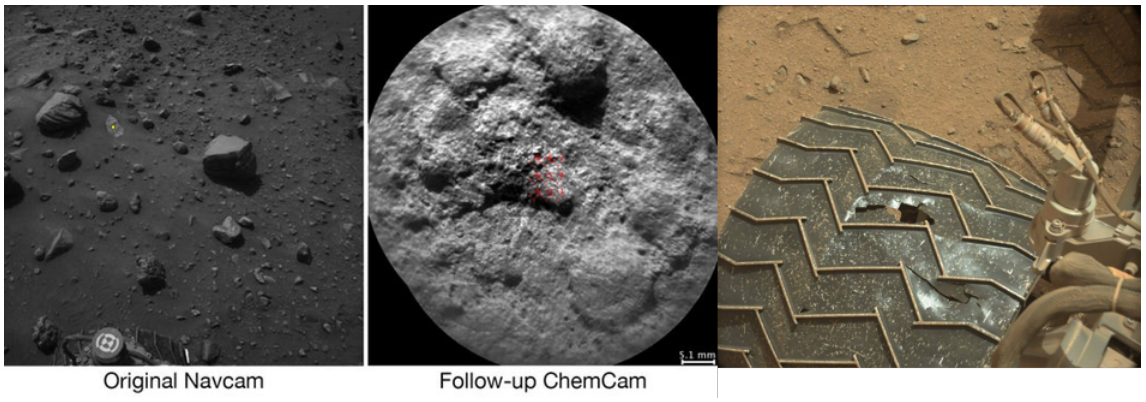

Figure 4: NASA's photos of Martian terrain from Curiosity

One of the most prominent features of Mars' surface is the large number of rocks of varying sizes. These rocks present significant navigational problems, as they need to either be driven over or avoided completely. There have been issues for Curiosity involving jagged rocks in the terrain, which have punctured and deformed its wheels as shown in Figure 4. The drivetrain and wheels form a vital subsystem on any robotic mining platform, since the mining operation depends on reaching the digging location. A major consideration in the development of a Mars rover should be to create a sustainable drive system to combat acute edges of Martian rocks.

For a mining operation, it is optimal to select a mining area that suits the platform's criteria. For example, a system ill-equipped to deal with the presence of large rocks should not begin mining in a rock-dense environment. In much of Mars' terrain there are many scattered varieties of rocks that will pose a challenge in mining operations. Therefore, there is motivation for implementing a maneuverable drive system coupled with a vision control system that will aid in guiding the rover through a preferable path to the extraction point, minimizing the potential damage along the way.

1.2.2 Atmosphere

The gravity on Mars is approximately one-third that of Earth's. This means that weight and consequently normal forces and friction should be designed to account for this difference.[10] Additionally, the composition of Mars' atmosphere is more than 95% CO_2 and less than 1% oxygen. This is drastically different than

[10]http://www.nasa.gov/audience/forstudents/5-8/features/nasa-knows/what-is-mars-58.html

Earth's atmosphere, which consists mainly of nitrogen (78%) and oxygen (21%).[11] Similarly, Earth has an atmospheric pressure of 101.3 KPa, while Mars has an atmospheric pressure of about 600 Pa, which is less than 1% of Earth's. These are all factors to consider when using motors, pneumatic devices, and other actuators, as the behavior on Earth will differ drastically from the behavior on Mars. In terms of temperature, Mars averages below -80 degrees Fahrenheit, which suggests the use of thermal protection for critical rover components. To maintain the health of the on-board electronics and battery, for example, it would be optimal to use some form of thermal protection. The specification sheets for most batteries show a declining battery life curve for colder environments. Furthermore, the lifetime of the components used must also be carefully evaluated, in order to ensure a mission failure does not result from a part reaching its end-of-life before the scheduled end of the mission.

1.3 Resources Available on Mars

In 2016 NASA published a study detailing the current state of Mars that started with an outline of the available resources, included current in-situ resource utilization (ISRU) technology, and concluded with an overview of plans for human habitation on Mars. ISRU refers to the capability to use the resources already available on Mars rather than needing to transport all necessary materials from Earth.Through discoveries made by Mars rovers and satellite imaging NASA has determined that the following resources are available. The polar icecaps on mars contain enough water to cover the entire surface of mars in a shallow ocean. Additionally there is evidence of large frozen lakes. While water concentration near the equator is only around 3% - 8%, the concentration rises to 40% or more at 60 degrees latitude. The presence of water also results in the the availability of water's constituents oxygen (O_2) and hydrogen (H_2). Regolith itself is highly oxygenated and can provide an additional source of O_2. With the carbon available in the form of CO_2 in the atmosphere, Mars has all the resources needed for creating plastics, methane and hydrogen fuels, and life support fluids. Nasa has also found evidence of metals, clay, and silicon dioxide (SiO_2), which is a main component of glass.[12]

[11] https://en.wikipedia.org/wiki/Atmosphere_of_Earth
[12] https://ntrs.nasa.gov/search.jsp?R=20160005963

1.4 The Robotic Mining Competition

A similar trend exhibited by all the currently deployed Martian rovers is the collection and analysis of Martian soil. However, all of these rovers have a limited digging depth, allowing them to only uncover material close to the surface; Curiosity, despite being the most recent rover to arrive on Mars, only has a digging depth of approximately 5 cm.[13] Given that the relative age of molecules increases with depth, Curiosity's quest for discovering the existence of life is decreased by hundreds of millions of years due to its 5 cm maximum digging depth. Furthermore, studies have shown that on parts of Mars, sheets of ice lie just below the surface layer of regolith.[14] In some cases, these ice slabs are estimated to extend downwards for over 40 m.

In 2010 NASA set a long term goal to "expand permanent human presence beyond low-Earth orbit."[15] In order to establish a presence on Mars, technology needed to perform ISRU needs to be developed. NASA established the Robotic Mining Competition to develop "technologies required to extract consumables such as O_2, H_2O, N_2, He, etc. for human life support replenishment."[16] This competition is designed for undergraduate college students from across the nation, and requires them to create robots to compete at the Kennedy Space Center in Florida. This technology will also be vital to advance the study of Martian geologic and biological history preserved below the surface. Given the incredible cost required to send cargo to Mars the first excavation robots will need to be compact, lightweight, and operate continuously with minimal human instruction to collect the necessary resources. Notably, on October 26, SpaceX held a press conference optimistically announcing that that they expect to send humans to Mars by 2023. Crucial to SpaceX's plan is ISRU in order to synthesize fuel for return flights from Martian ice.[17]

1.4.1 The Competition

To simulate a Mars-like environment and scenario, RMC robots must fit within the starting dimensions 0.75 m x 1.5 m x .75 m, weigh less than 80 kg, and be electrically powered - this constraint is to mimic the minimal space that rovers must

[13] https://www.wired.com/2012/07/why-curiosity-needs-to-dig-deep-for-organic-molecules-on-mars/

[14] http://www.space.com/30502-mars-giant-ice-sheet-discovery-mro.htm

[15] https://www.nasa.gov/sites/default/files/files/Olson_NACCapabilityDrivenRoadmap030612_508.pdf

[16] http://www.nasa.gov/sites/default/files/atoms/files/rmc2017_02_message_projectmanager_rev01_09152016.pdf

[17] http://www.spacex.com/sites/spacex/files/mars_presentation.pdf

occupy during transit to Mars. The competition field is comprised of a top layer of Black Point-1 (BP-1) Martian Basaltic Regolith Simulant that is 30 cm deep, which covers a 30 cm layer of gravel. The gravel is a stand-in for ice believed to be below the surface on Mars. Robots score points after collecting and depositing at least 10 kg of regolith or gravel. Robots are awarded three points per kilogram of regolith deposited. As gravel represents ice, it is much more valuable and a kilogram of gravel is worth 15 points. The field, shown in Figure 5, has major dimensions of 3.78 m x 7.38 m and is broken into three sections. The starting zone is 1.5 m long and includes two sub-zones, each of which is 1.89 m x 1.5 m. The robot begins the match in a randomly selected zone and with a random orientation. Along the wall in the starting zone is the trough for depositing regolith and gravel. The edge of the trough is slightly behind the back wall and is approximately 0.55 m above the regolith. The trough, as shown in Figure 6, has tapered edges and a screen that separates the gravel from the fine regolith particles. Beyond the starting zone is a 2.94 m long obstacle area. Included in the obstacle area are two craters with a maximum width and depth of 30 cm and three obstacles. The obstacles have a diameter between 10 cm to 30 cm and weigh between 3 kg and 10 kg. The robot is prohibited from collecting regolith inside of the obstacle area. The mining area is the final section and is 3.78 m x 2.94 m. Material may only be extracted in the mining area, and must be transported to the trough in the starting zone to be scored.

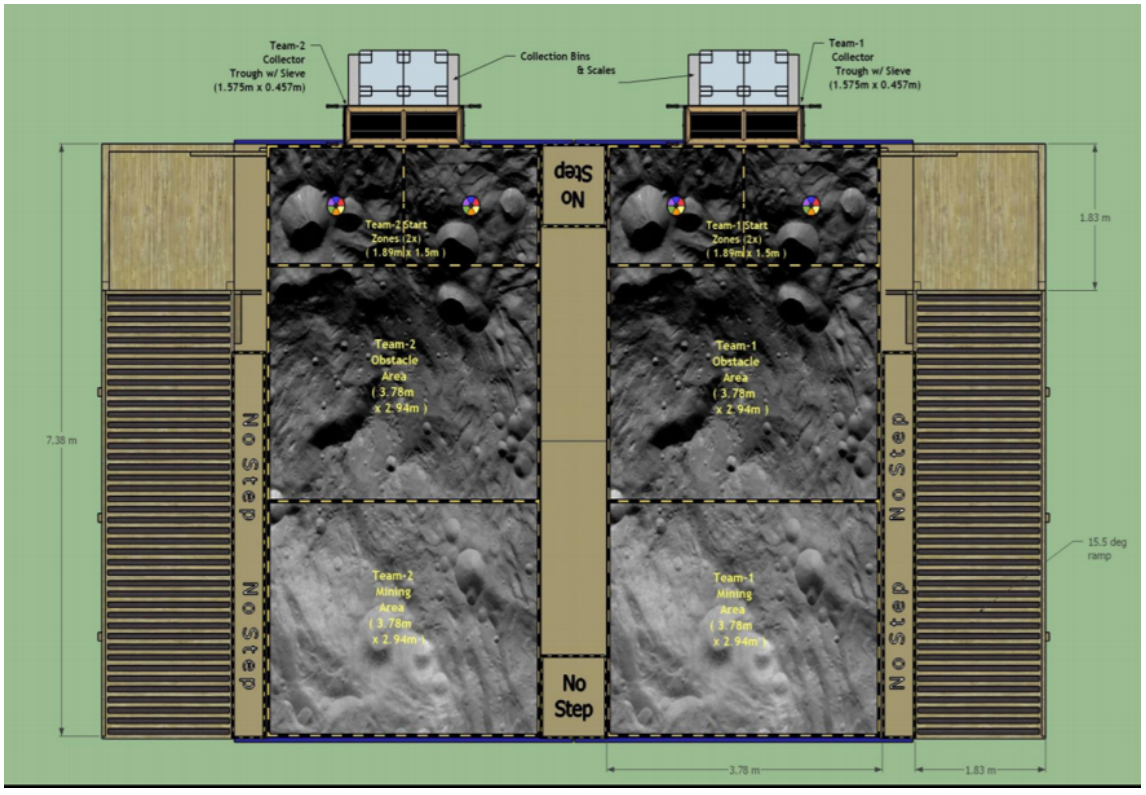

Figure 5: RMC field layout and dimensions

[18]

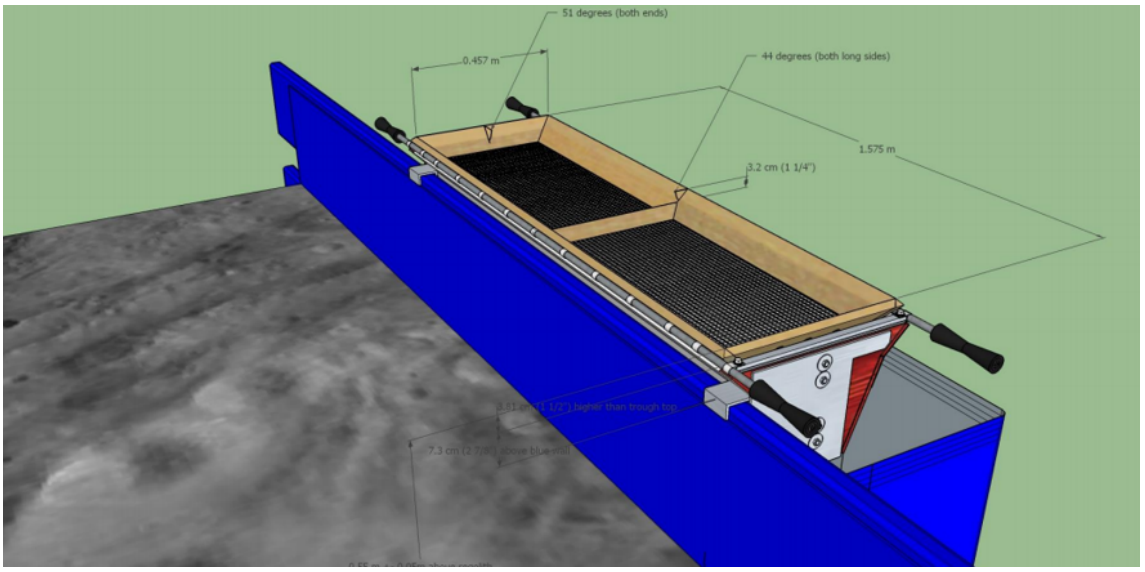

Figure 6: Collection Trough

Robots can gain additional points for dust tolerant design, dust free operation, and autonomy. While each competition run lasts only 10 minutes, a robot on Mars would have to operate for months or even years without maintenance. Dust free operation is necessary to keep the robot performing at peak efficiency, as mechanics are not available for repairs if the robots are sent in preparation for humans to arrive later. Furthermore, the robots created for this competition are not expected to be actually deployed to Mars, but are required to only use technologies that would function on Mars. For example, using a GPS for navigation is prohibited, as no positioning satellites are in orbit around Mars.

1.5 Existing Solutions to Resource Collection

The excavation of materials below the surface is a difficult problem, but not a new one. Earth based mining is an established industry, but mining on Mars introduces new challenges due to size, weight, and power constraints of the machines that can be launched into space. A significant amount of research and development has been done to discover the best method to collect buried material. This section outlines several common collection schemes, including the use of a bucket wheel and a conveyor system.

[18] http://www.nasa.gov/sites/default/files/atoms/files/15rmc2017infographics.pdf

1.5.1 Bucket Wheel

A bucket wheel excavator is one method commonly used for continuous digging in open mining. Buckets are attached to a large wheel, and as this wheel spins, the buckets pick up soil and rock. The Bagger 293, one large-scale example of a bucket wheel system, can carry 1452 gallons of material in each bucket, similar to the wheel shown in Figure 7.[19]

Figure 7: Bucket Wheel Excavator

[20]

The main base of the Bagger 293 is stationary as the bucket-wheel excavates level-by-level in arcs through the dirt. During normal operation about a quarter of the buckets on the wheel are in contact with the dirt at any given time. Additionally the wheel itself never digs deeper than the buckets on the wheel. A number of groups have imitated the bucket wheel excavator on a smaller scale for Martian and lunar excavation. Astrobotic Technology Inc. in Pittsburgh designs robots and landers capable of lunar missions, including mass excavation and planetary exploration.[21] They have designed a compact rover with a bucket wheel perpendicular to the drive wheels, as shown in Figure 8.

[19] https://www.pexels.com/photo/bucket-wheel-excavators-open-pit-mining-brown-coal-garzweiler-33192/

[20] https://www.wired.com/2009/10/giant-gadgets/

[21] https://www.astrobotic.com

Figure 8: Image of Astrobotic's Lunar Excavator

[22] A video published by Astrobotic Technology[23] shows a test run of their robot operating. The orientation of the digger allows the robot to dig a wide trench as it drives. However, the trench the robot digs is only a few centimeters deep, and never digs deeper than the buckets. A team of students competing in the 2016 NASA Robotic Mining Competition built a bucket wheel system that both dug and acted as one of the drive wheels. This robot's excavation is significantly more aggressive than Astrobotic as it can dig to a depth that is close to the radius of the bucket wheel.[24] The dirt slides out from the center of the wheel through a chute into a bucket on the side of the robot. The side bucket rests on the surface of the dirt, and can rotate vertically to transfer dirt to a larger compartment inside the bucket. This system limits the depth the digger can reach as the entire wheel cannot be fully submerged. This specific digger configuration is likely incapable of reaching the gravel below the surface regolith. Another variation of the bucket wheel is for the wheel to also act as the container that holds the regolith and gravel. NASA uses this approach in their RASSOR excavator, shown in Figure 9.

[22]https://www.astrobotic.com/assets/recruiting-24eaa351e15a8b120662647469993ae0.jpg
[23] https://www.youtube.com/watch?v=bzY3M3tYLHk
[24]https://www.youtube.com/watch?v=WSoiOBIThuk

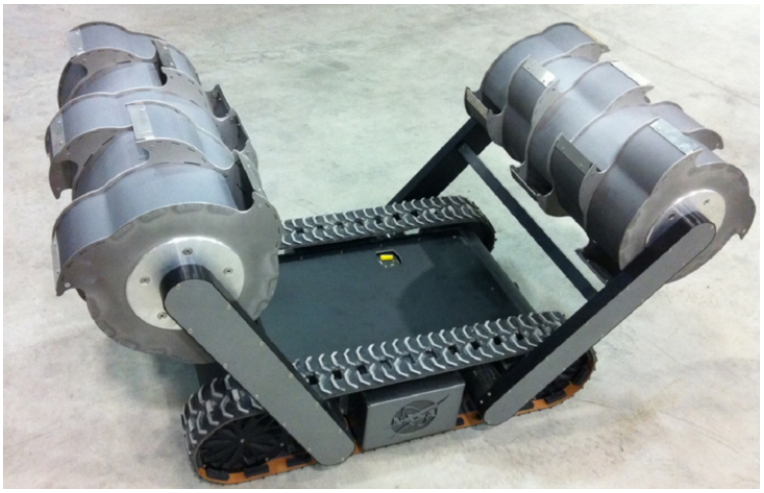

Figure 9: RASSOR Excavator

[25]

This design reduces the complexity of the bucket wheel system as the regolith does not need multiple stages to transfer material into the unloading station after being collected. As of 2015, the RASSOR can carry a maximum of 20 kg of regolith, and weighs around 100 kg. This method of digging could reach the depth of the gravel, but would likely need multiple trips to deposit the collected material. The shape of the bucket limits the overall volume that the robot can carry at once. Additionally this containment system requires high torque during the dumping phase as the regolith container is extended on a lever greater than the radius of the wheel.

1.5.2 Conveyor Mechanism

In addition to the bucket collection method, another commonly implemented collection mechanism is a conveyor system that has scoops on it. A key benefit of this system is its simplicity and ease of implementation in different robot designs. In fact, over half of the teams participating in the Robotic Mining Challenge have used a collection system that falls into the conveyor category. This system is used by industrial trenchers (shown in Figure 10). The trencher is used to remove large amounts of material in order to dig trenches for pipes and electrical cables. One point worth noting is that the trencher is generally used for simply removing material and does not normally collect the excavated material.

[25]https://technology.nasa.gov/patent/KSC-TOPS-7

Figure 10: Conveyor-based trenching system

[26]

The majority of the RMC teams that have implemented this system in previous years have used a simple approach where buckets are attached to a driven chain. This collection mechanism is then lowered to a point where it can mine regolith. The system is efficient, continuous, and robust, but has drawbacks. For example, many implementations unreliably transfer material from the bucket scoops to the main storage (sometimes dumping onto other components or back onto the ground). The main challenge lies in positioning the buckets in an orientation that guides the material into the main storage without adding too much complexity. WPI's Moonraker robot, shown in Figure 11, implements a five shaft system as a solution to the dumping issue. Moonraker's collection system was designed to control the orientation of the buckets at specific positions. The buckets will only ever dump material after reaching a reasonable position over the main storage unit. Moonraker and many other robots that we observed were mainly designed to collect within the upper layer of regolith; most do not even attempt to mine the gravel on the lower layer.

[26]http://www.boxerequipment.com/wp-content/uploads/2015/01/Boxer-120-cutout-980x551.jpg

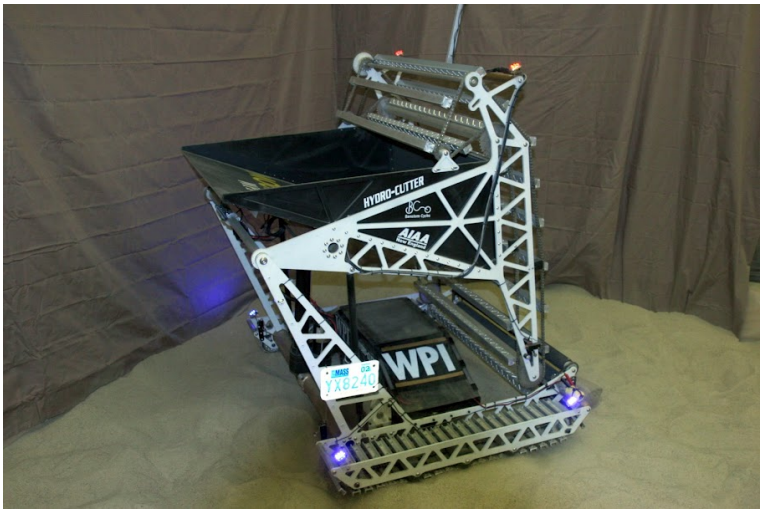

Figure 11: Moonraker preparing to collect material

The conveyor collector system requires a second mechanism to dump the material collected. There are three primary ways that this has been done in the past which are:

1. a second conveyor system dedicated to dumping the material,
2. a bucket that dumps the material into the collection area, and
3. an integration of a bucket into the collector conveyor

All three methods have different advantages and disadvantages. A dumping conveyor, for example, will take a lot longer to dump than a dumping bucket (as the conveyor gradually deposits material instead of all at once), but will require less torque to complete the operation. Similarly, integrating a dumping mechanism into the collecting conveyor will require a great deal of torque to actuate and can likely lead to robot stability issues if completed incorrectly.

2 Methodology

In order for this project to be a success, significant planning and budgeting was needed to complete the robot on time. The team began working on the project at the start of WPI's 2016 school year (August 25th), and planned to finish the project at the beginning of May 2017, leaving a week or two of leeway before the competition. The core phases and milestones of the process are outlined below:

- Brainstorming and Research
- Milestone: System Requirements
- Milestone: Robot Plan of Operation
- Prototyping
- Modeling and Design: Phase 1
- Milestone: Preliminary Design Review
- Budgeting
- Modeling and Design: Phase 2
- Manufacturing
- Testing
- Milestone: Critical Design Review

2.1 Brainstorming and Research

Instead of immediately rushing into the prototyping phase, a significant amount of brainstorming and research was done in advance to ensure that all design decisions were made with a compelling rationale. The first several weeks of the project were dedicated to learning more about the challenge through a variety of mediums. Several research papers about traversing granular materials were identified and contributed heavily to the drive system the team created. Furthermore, videos on YouTube depicting other teams' designs and attempts at previous Robotic Mining Competitions were viewed; these allowed the team to identify effective methods for collection and material release. Using this information, through a series of design meetings the team developed various rudimentary sketches of potential robot designs, such as the one shown in Figure 12.

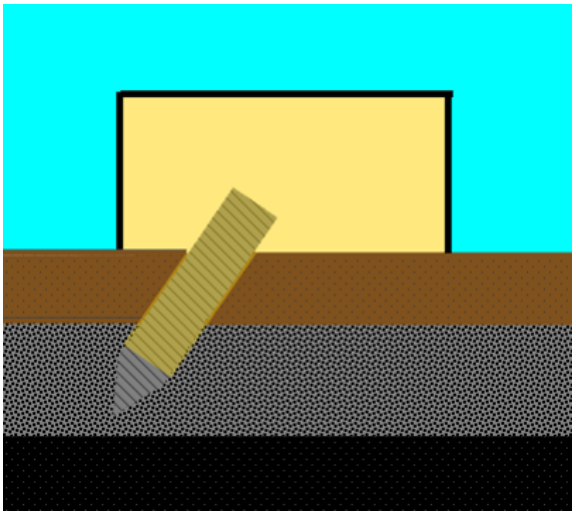

Figure 12: Early electronic sketch of a robot with retractable digging system

2.2 Milestone: System Requirements

Following the brainstorming sessions, the team then outlined the requirements the system would need to be successful. The design requirements are shown in Table 1.

Maximum Size	1.5 m × 0.75 m × 0.75 m
Maximum Weight	80 kg
Battery life	10 minutes
Payload Capacity	Capable of transporting at least 50 kg of combined BP-1 and gravel in a single payload.
Material Collection	Capable of collecting at least 100 kg of combined BP-1 and gravel within a 10-minute time frame.
Gravel Collection	Capable of collecting at least 20 kg of gravel within a 10-minute time frame.
Control	Capable of executing autonomous subroutines (such as driving to a specific location or collecting a full payload).

Table 1: Design Requirements

Some of the requirements in this table were specifically specified by NASA, such as the maximum size and mass of the robot. Others, such as Payload Capacity and Material Collection were identified by the team as specifications that would be necessary for a robot that excels in the competition.

2.2.1 Maximum Size

The maximum size of the robot is 1.50 m (l) x 0.75 m (w) x 0.75 m (h). These dimensions are set by the RMC and define a reasonable, compact space that a robot being deployed to Mars should occupy. This is a moderately sized robot compared to those already deployed to Mars - Sojourner was relatively small with a bounding box of 0.66 m (l) x 0.48 m (w) x 0.30 m (h); Spirit and Opportunity were medium sized rovers with sizes of 1.60 m (l) x 2.30 m (w) x 1.50 m (h); Curiosity is the largest with a size of 2.90 m (l) x 2.70 m (w) x 2.20 m (h).

2.2.2 Maximum Mass

The maximum dry mass of the rover is 80 kg, as specified by the RMC. This mass, similar to the size, falls in the middle of the masses of the existing Mars rovers: Sojourner is 11.5 kg, Spirit and Opportunity are 185 kg, and Curiosity is 899 kg. It should be noted that 80 kg is an absolute maximum; the design implemented by the team conserves weight wherever possible to minimize the dry mass of the system. As the weight of the rover increases, so does the amount of fuel needed to propel the robot.

2.2.3 Payload Capacity

The minimum capacity of regolith and gravel that the rover should be capable of carrying is 50 kg. Having a high carrying capacity reduces the number of trips to the collection bin. Therefore, in order to collect the desired amount of material in a ten-minute period (100 kg), the robot should need to make no more than 2 trips to the collection station. Increasing the payload capacity reduces the amount of time spent traversing between the digging zone and the collection station.

2.2.4 Material Collection

The rover must be capable of transporting at least 100 kg of combined regolith and gravel within a ten minute period. This means that either a single 100 kg collection trip will be made, or two collections that sum to 100 kg will be made. This value was selected based on results from previous occurrences of the Robotic Mining Challenge; the top teams have collected nearly this much material.

2.2.5 Gravel Collection

One of the key goals of this rover is to collect the gravel below the regolith. In order for this project to be deemed successful, the robot should be capable of collecting at least 20 kg of gravel within the 10-minute time frame. This puts a significant emphasis on gravel collection and will require the digging mechanism to be robust enough to repeatedly dig and collect the gravel below a depth of 30 cm.

2.2.6 Control

The robot must be capable of executing subroutines with autonomy. In a scenario where this rover was actually deployed to Mars, it would be impossible to use completely teleoperated control due to extreme signal latency between Earth and Mars. Therefore, being able to issue a single command that begins an autonomous routine is necessary. Some candidates for autonomous subroutines include driving to or from the digging location, digging to a fixed depth, or dumping the payload at the collection site. The system must also be able to troubleshoot problems during subroutines. For example, if an object is lodged between the sprocket and chain, then the robot should perform a series of operations to identify where the problem has occurred and attempt to dislodge the object before resuming the main operation. This would increase overall task efficiency and reduce the time it takes to wait for commands from the control station.

2.3 Milestone: Robot Plan of Operation

In order to successfully complete the Robotic Mining Challenge, a strategy for the robot's operations is crucial. The remainder of this section outlines the key stages of the robot's operation and specifies the information the robot must know at each stage.

2.3.1 Achieving a Known Orientation

As per the rules of the RMC, the robot will be placed in one of two starting zones and will be assigned a random rotation. The robot will have an autonomous routine that allows it to establish a known orientation. This will be accomplished by placing a passive beacon (like a sign or lights)in front of the collector bin. The robot will use a camera to detect the beacon; once the beacon is located, the robot

will be able to derive its orientation from the viewing angle of the beacon. After acquiring a known orientation, the robot will rotate until it faces the mining area of the field.

2.3.2 Driving to the Mining Area

After rotating to an appropriate orientation the robot will begin to drive towards the mining area. The robot will push through all obstacles (rocks on the surface). The robot will actively keep track of its distance from the collector bin, as well as looking for the painted orange line that denotes the digging zone. Once the robot is confident that it has entered the digging zone, it will continue driving forward for a set distance in order to dig the hole as close to the far wall as possible. When the robot arrives at the correct digging location, the drive motors will stop.

2.3.3 Mining Regolith and Gravel

Once the robot is stopped, the collection mechanism will be lowered and material will begin to be collected. It is important that the current depth of the mechanism is known, as well as the speed at which the scoops are moving (so they can be controlled via PID). The load on the motors also needs to be sensed which will indicate if the scoops are actually contacting material. Furthermore, the robot will sense how much material has been collected, so that it will know when to begin its path back to the dumping station. Once the bucket is filled, the scoops must be retracted from the ground, and the position of the bottom scoop must be known in order to avoid scraping the scoop on the ground on the return trip. During the process, the robot should minimize the dust produced and should ensure that it is not digging in an area that it has previously excavated from.

2.3.4 Driving to the Collection Bin

After the robot has collected all of the necessary materials, it will begin driving in reverse to the collection bin (it never rotates after discovering its initial orientation). The robot will ensure it follows the same procedure it used when driving to the mining area: drive straight. There will be feedback as the robot approaches the collection bin to ensure it aligns itself perpendicularly with the bin. Furthermore, it must ensure the back of the robot is flush with the collection bin. Once these requirements have been met, the robot can begin to dump the material.

Figure 13: Early models of the collection scoops

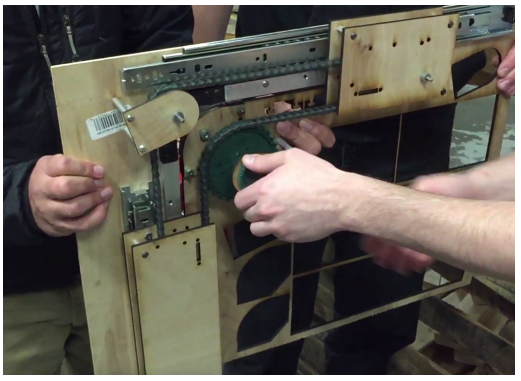

Figure 14: Prototype of the dynamic chain collection system

2.3.5 Dumping Material

The robot is capable of sensing the angle and angular velocity of the bucket. It is also capable of sensing that the bucket is empty, so that it knows when to lower the bucket back to its traveling configuration. If the robot has more time to continue excavating after the completion of the dumping routine, the same sequence of subroutines will be performed until time expires (starting with "Driving to the Mining Area.")

2.4 Prototyping

For any project to be successful, ideas must first be tested before being implemented in their final form. $1,000 was allocated towards constructing prototypes and testing designs. Through prototyping, important realizations were made regarding the construction and operation of the robot's subsystems. For example, scoops and the means of lowering them into the ground were tested in advance with wooden prototypes, as shown in Figures 13 and 14. Appendix C provides additional examples of prototype and testing rigs.

2.5 Modeling and Design: Phase 1

Towards the end of the Prototyping phase, the team began creating CAD models of the robot. This phase was largely dictated by the Preliminary Design Review (PDR), which was scheduled for December 1st. Therefore, the goal of this phase was to use the information obtained from research and prototyping to create the basis

for the final robot. This model was expected to change significantly as information obtained from the PDR was considered, but needed to be complete enough to convey our goals and ideas to those in attendance at the presentation. Figure 15 shows the model of the robot that was presented during the PDR.

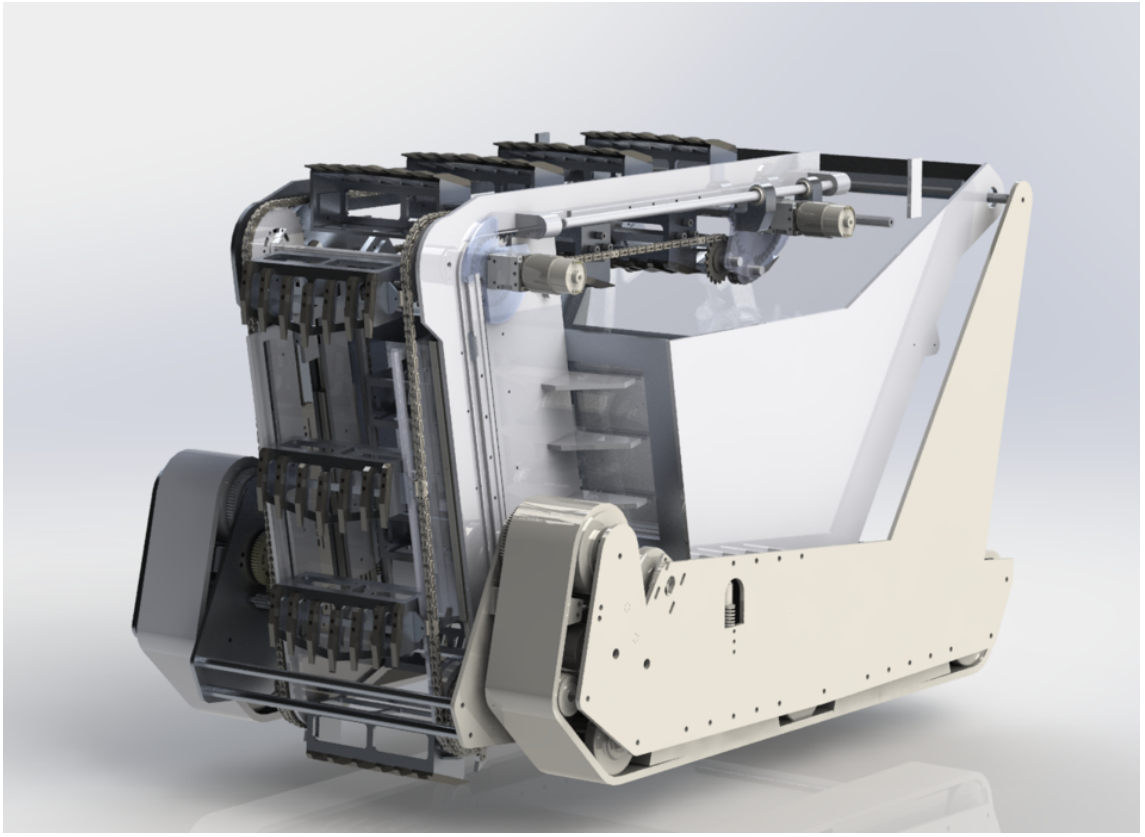

Figure 15: Early CAD model of the robot

2.6 Milestone: Preliminary Design Review

The PDR was presented on December 1st, 2016. In attendance were the entire team, the project advisors, faculty from the Robotics Engineering Program at WPI, and fellow WPI students. The PDR provided a time to validate and discuss design ideas for the robot. While most of the design had been finalized, the PDR provided a chance for a peer review of the decoupling of the bucket and collection mechanism as shown in Figure 16. A peer review of this concept was important because this design has not previously been implemented by any competition participants.

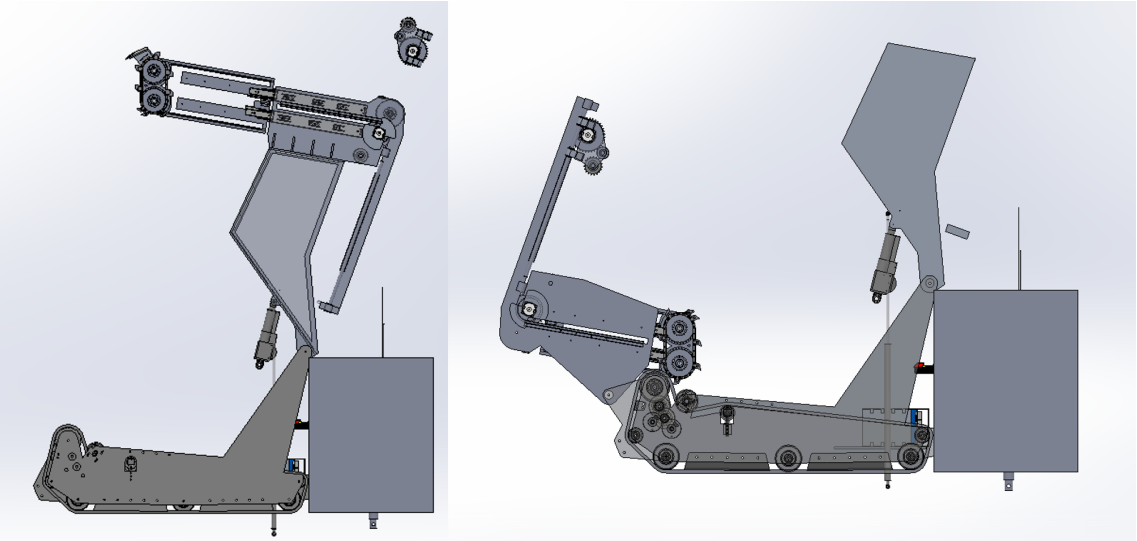

Figure 16: Decoupling the collection system from the material release system

2.7 Budgeting

With a preliminary model of the robot in place, costs of the various subsystems could be estimated. In order to create an accurate budget, every part included on the model of the robot was accounted for and had an associated price. This information was all compiled into a spreadsheet to calculate the bare-minimum cost for the parts. To arrive at the final budget, a shipping cost buffer, an unexpected-costs buffer, and travel costs were added. Table 2 shows the breakdown of the budget for each of the subsystems.

Markhor Overall Budget	Totals
Drive System	$3,619.86
Collection System	$1,864.11
Dumping System	$772.53
Electrical System	$718.02
Travel & Misc.	$1300
Subtotal	**$8,274.52**
Safety Factor 5%	$413.73
Subtotal	**$8688.25**

Table 2: Robot Budget

Ultimately, the budget for the robot was set at $8,750. Most components needed for the robot were acquired from popular retailers like McMaster Carr, AndyMark, Amazon, and Cross The Road Electronics.

2.8 Modeling and Design: Phase 2

The PDR and budget were both used to guide the continuing development of the robot. Eventually, the final design of the robot was created, as shown in Figure 17.

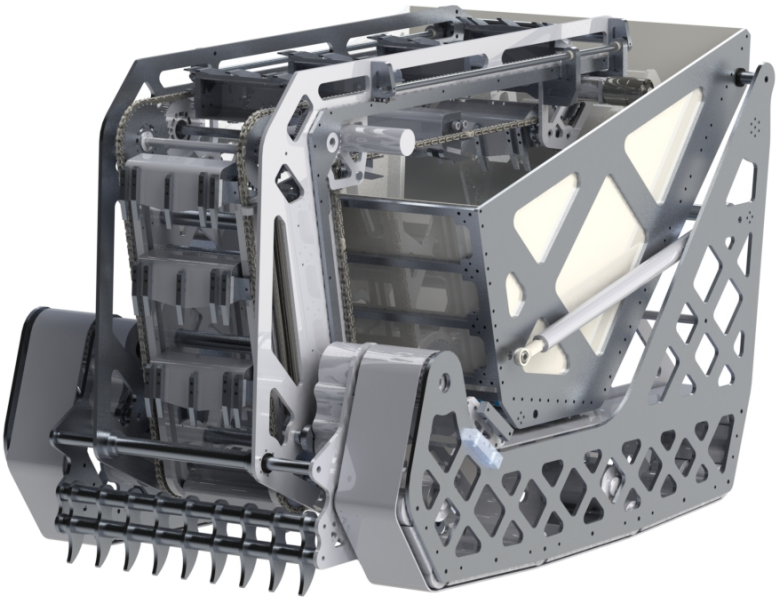

Figure 17: Final model of the robot

While the robot does not appear drastically different the Phase 1 model (Figure 15), a significant number of changes were made. These changes include decoupling the collection and material release systems, adding weight saving cutouts, a re-design of the collection scoops, and various other improvements. In designing the final model of the robot, completing certain subsystems was prioritized. For example, the locomotion subsystem was finished first; this allowed this subsystem to be physically constructed while the rest of the design was in progress.

2.9 Manufacturing

As mentioned earlier, manufacture of the robot occurred concurrently with the second phase of Modeling and Design. Whenever possible, parts were machined by the team using the Washburn Machine Shop at WPI. Virtually every custom part was made by the team, with the exception of the large plates that form the structure of the robot (these parts were sent off site to be machined with a water-jet). In total, about 300 parts were created, machined, and assembled by the team. Appendix D includes a sample of parts manufactured in Washburn.

2.10 Testing

Testing of the different systems that make up the robot was an ongoing process. As subsystems were manufactured and put together testing was able to be done with them in order to work out any flaws. Full scale testing began when the robot was fully assembled. Testing included drive and localization testing, digger tests while driving, and material dumping tests. Testing continued after Project Presentation Day until the robot was transported to Florida for the competition.

2.11 Milestone: Critical Design Review

The Critical Design Review was on April 20th. The presentation covered the process of prototyping, designing, manufacturing, and testing the robot. Furthermore, it covered the results of the testing and what the team could have improved. The presentation was presented to the project advisors, faculty from the Robotics Engineering Department at WPI, and any WPI students who wished to attend.

3 Mechanical System

3.1 Locomotion

3.1.1 Design

The drive system for MARKHOR consists of two tread-based modules. Each module measures approximately 13.7 cm x 25 cm x 89 cm (5 in x 10 in x 35 in). A side view of one of the drive modules is shown in Figure 18.

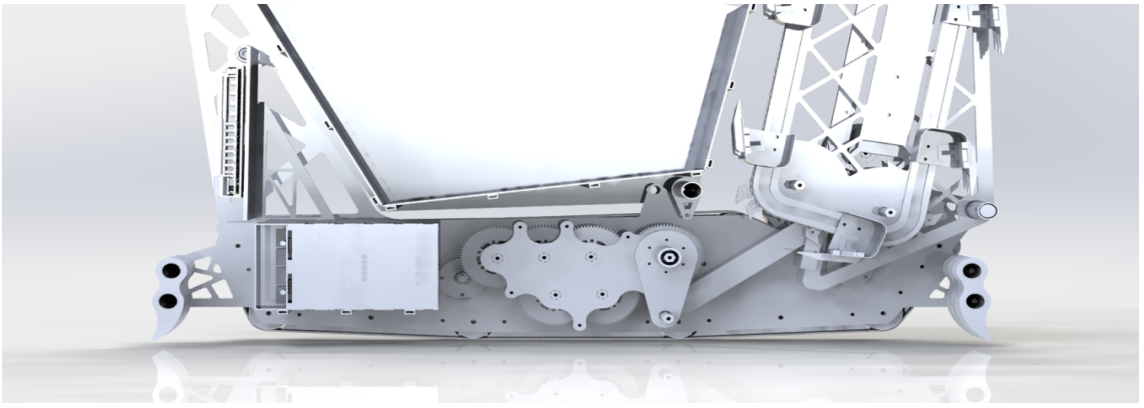

Figure 18: Side view of a drive module

Each module features a 0.635 cm (0.25 in) aluminum frame with weight saving cutouts; this thickness provides enough strength to support the maximum weight of the robot with a 100 kg load (∼220 lbs), while also minimizing weight to comply with the 80 kg design requirement.

Treads

Each tread in the drive subsystem is a 2.31 m BRECOflex ATK10K13 timing belt. A variety of options were considered for the type of belt that would be used, but eventually the ATK10K13 was selected. This belt features a strong serrated, molded track that guides the belt along the sprockets and pulleys. This eliminates the need for additional flanges on all of the sprockets and pulleys. The tread has a herringbone pattern to provide the robot sufficient traction to drive without stalling the motors from friction while turning. The herringbone pattern belt is shown in Figure 19. This model was desirable because it would most-evenly distribute the weight of the robot across the entire tread, instead of focusing the weight on several points. The primary alternative option was to use a tread similar to the one shown in Figure 20. However, this option was ultimately ruled out because if one or more

of the weld-on profiles broke, the tread would have an area where it could not drive, rendering the system useless.

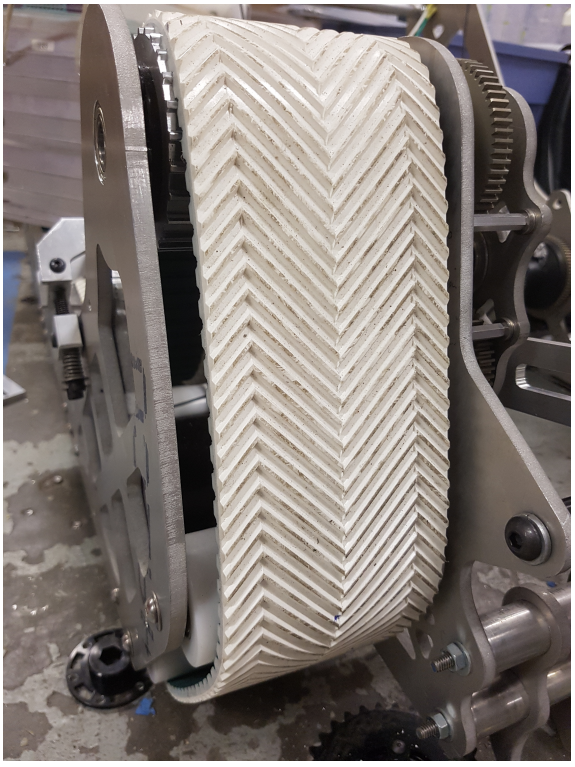

Figure 19: Belt with herringbone pattern

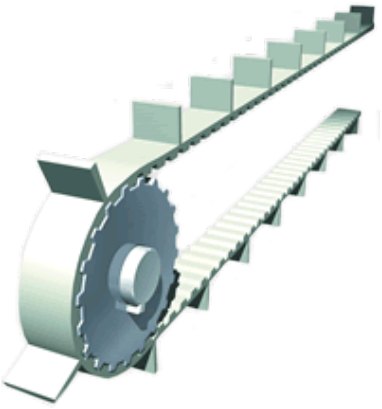

Figure 20: Belt with weld-on profiles

Another important design decision in the creation of the drive modules was the placement of the driven pulley. Based on a prototype drive system, the belts would become jammed if too much regolith or gravel was caught between the drive pulley and the belt itself. The following measures were taken to prevent belt binding. First the drive sprocket is elevated off the ground to prevent debris from getting between sprocket teeth. Any regolith or gravel that enters the system will fall out

and be prevented from reaching the drive pulley. Additionally each drive module also features a compliant tensioning system, shown in Figure 21.

Figure 21: Compliant tensioning system on one of the drive modules

Belt Strength

The main specifications that were considered when selecting a belt were its strength, specific belt mass, back bending capabilities, belt pitch, and belt friction. The belt's strength was a key specification to consider; in order to have a robust drive system, the main component of the system responsible for driving cannot be allowed to break under a reasonable load. An example situation that would cause a belt to break would be when the robot is carrying a full payload and turning in place. The robot is also at a heightened risk of breaking a belt if it is pushing a heavy object and is stalling out. The herringbone backing pattern was chosen for the exact purpose of limiting the harmful effects in both of these cases. With the herringbone pattern, the drive track is more likely to skid in place than rip the belt since it is operating in a regolith particle environment.

Even so, calculations were performed to ensure that the belt would not break if operating in a different environment that had a higher friction coefficient between the belt and ground surface. With the ATK10K13 belt, the breaking strength is 8500 N. A drive pulley with a diameter of 80 mm and 25 tooth count of was chosen (shown in Figure 22), which would have to apply 675 N-m to break the belt. With the CIM motor that was chosen to drive the system, this would require a gearbox of 279:1 since the stall torque of the motor is 2.42 N-m, compared to the 75:1 gearbox

chosen. This give the system a factor of safety of 3.7. The drive pulley size was chosen to ensure that with ∼180 degrees of belt wrap there would be enough teeth in contact so that the chance of a single tooth breaking under high forces was limited. Belt pitch was chosen to be a compromise between belt stiffness and toughness. Typical BRECOflex belts are available in 5 mm, 10 m and 20 mm pitch options. The greater the pitch, the greater the strength, but the stiffer the bending properties are. Additionally, specific belt mass increases with belt pitch. The middle option was chosen in order to achieve a lightweight but strong drive system.

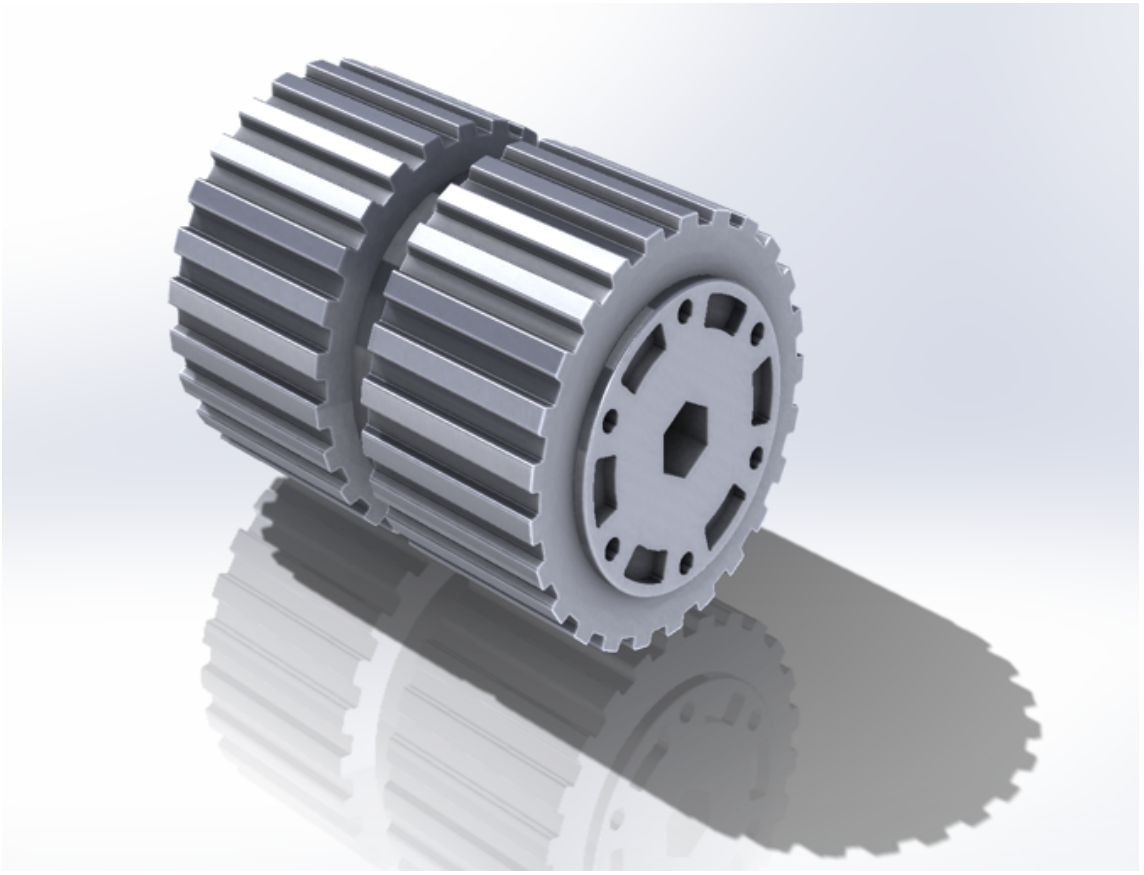

Figure 22: 25 tooth pulley used for driving the belts

The chosen ATK10K13 belt is specified for 15 teeth in normal operation and 120 in back bending. This translates to pulley diameters of 48 mm and 381 mm. The bending in normal operation was satisfactory for the drive system, but the back bending diameter was very large, so a custom roller was designed instead of a round pulley. The custom roller module gives the same performance of a pulley that is 120 mm in diameter while being very compact by utilizing only the ∼40 degrees of wrap that is put on it.

Tension Modules

Compliance has been added to the system in the form of dynamic tensioning. A set of compression springs and a series of Delrin rollers are used to keep the belt in tension. This system allows the tension on the belt to be slightly relieved if a rock was to pass through the drive rollers, and will be immediately restored to the original tension after the rock exits the system. The location of the compliance system also ensures that the drive pulley always has 160 degrees of wrap, which prevents the belt from slipping on the drive pulley. As previously stated, because the BRECOflex timing belts have a minimum wrap diameter on the non-cleated sides, the tensioners were designed to have multiple rollers to compensate for this limitation.

Gearing

The desired drive speed of the robot was ~0.23 m/s. Each module was built with a 12 V CIM motor contained within the drive module. The output of this motor is connected to a custom 4 stage, 75:1 gearbox. Based on the motor curve for the CIM motor (shown in Figure 23), the ungeared motor is expected to run at 3700 RPM and therefore produce 0.55 Nm of output torque.

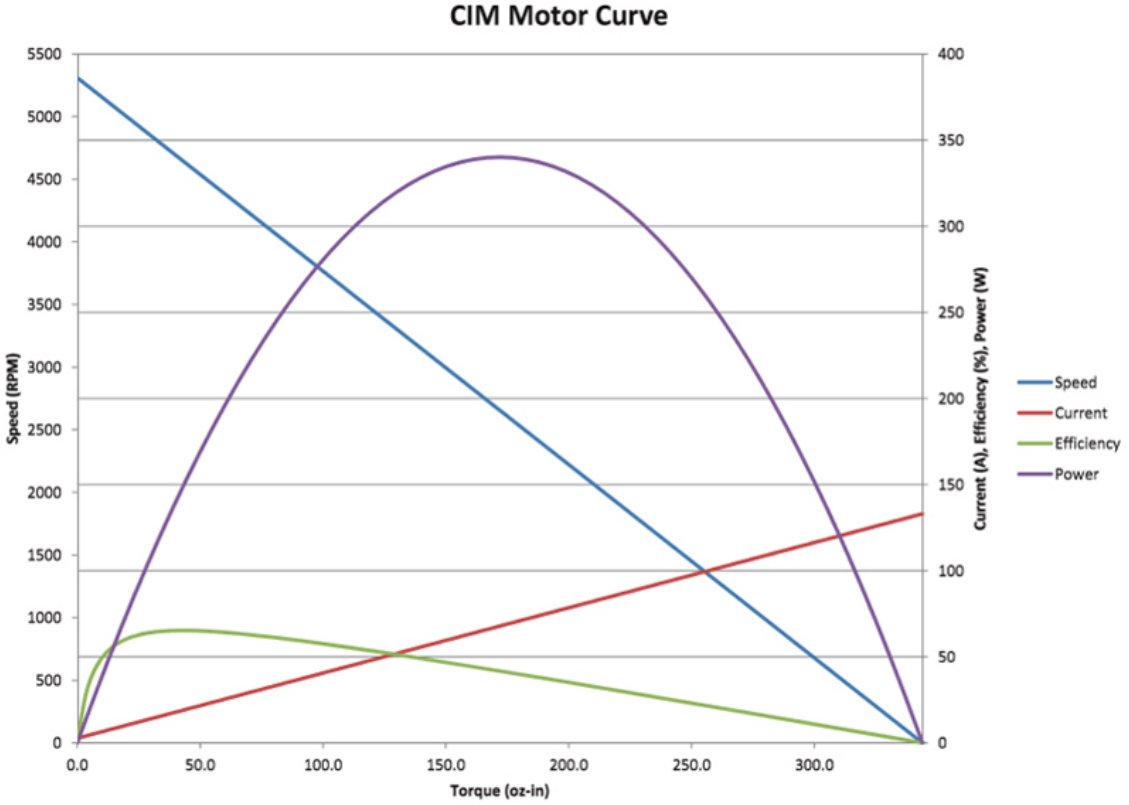

Figure 23: Speed-Torque-Power curve for the CIM motor

Dust and Rock Protection

Because this rover is designed to work in a potentially dusty environment, several measures were taken to prevent dust or rock related damage to the drive system. The drive modules are covered by polycarbonate sheet, which prevents most dust and rocks from entering the drive system. Between each of the drive rollers is a custom Delrin block that serves the dual purpose of evenly distributing weight and preventing rocks from entering the system. As mentioned before, in the event that a loose rock manages to enter the system, the tensions module is designed to prevent damage to the belt. Furthermore, each gearbox is protected by a custom 3D printed case that completely seals the gearbox. The polycarbonate sheets and gearbox housings are both easily removable to allow for maintenance of the drive modules.

3.1.2 Analysis

Worst Case Scenario

The first step to determining the power requirements for the drive system involves understanding what situation the robot would need the most power in. In an ideal scenario, the robot will only need to drive straight, in which case the constraints are minimal. However, given the environmental challenges, the robot may experience driving on slopes and potentially be forced to rotate due to unfavorable conditions. Figure 24 below shows a flowchart that describes the considerations for worst case scenario. The final decision ended up being the case where the robot is fully loaded while driving straight on a sloped surface.

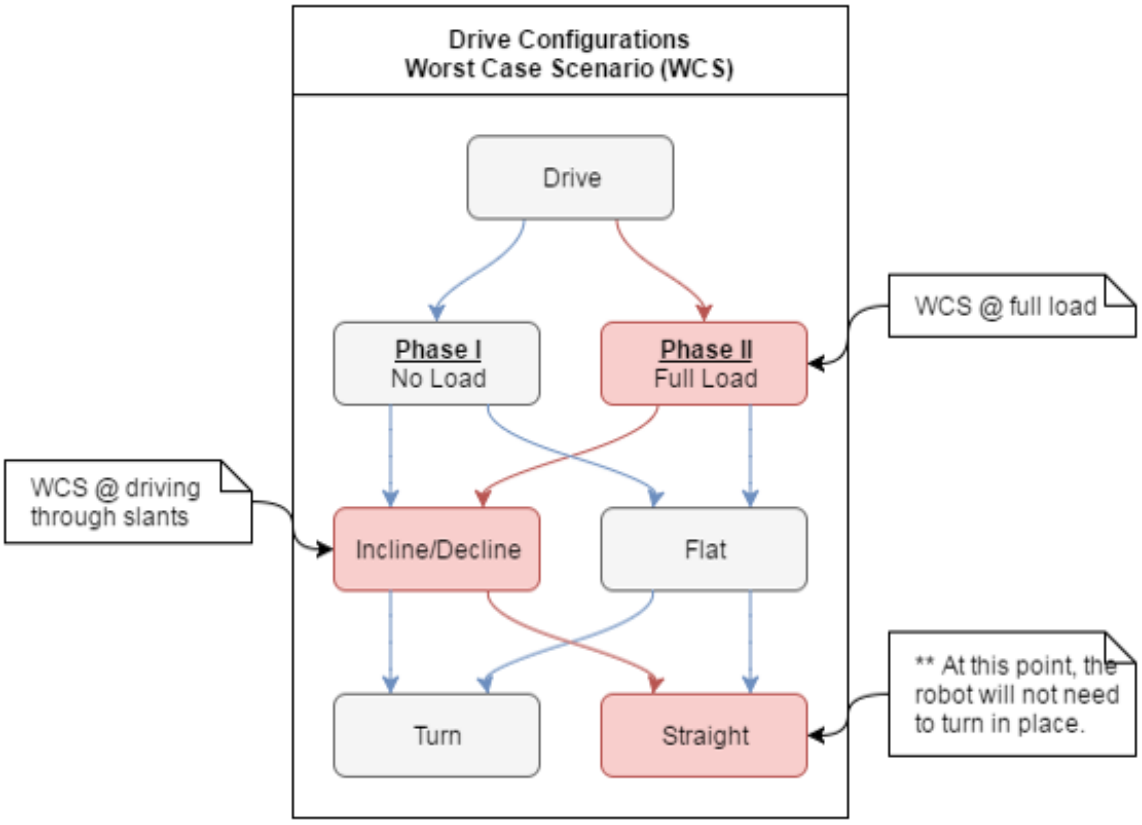

Figure 24: Worst Case Driving Scenario Decision Tree

Power Requirement

The drive motor calculations were performed with these considerations in mind. At worst case, the robot will be carrying 100 kg of material and driving up a 30° incline. The incline estimation was based on observations of previous RMC field conditions. The next design decision was the operating speed under these conditions. The desired final speed was 9 in/s. Factoring in gear inefficiencies and friction due to bearings, dust, etc., the required torque came out to be 37.6 Nm. Thus, using these values, the power requirement is approximately 236 W. The gear ratio required to meet these specifications was calculated to be 75:1 with a current draw of 32 A. Figure 25 below provides a visual representation of how the parameters of the system change with respect to the output torque of the motor to achieve these specifications.

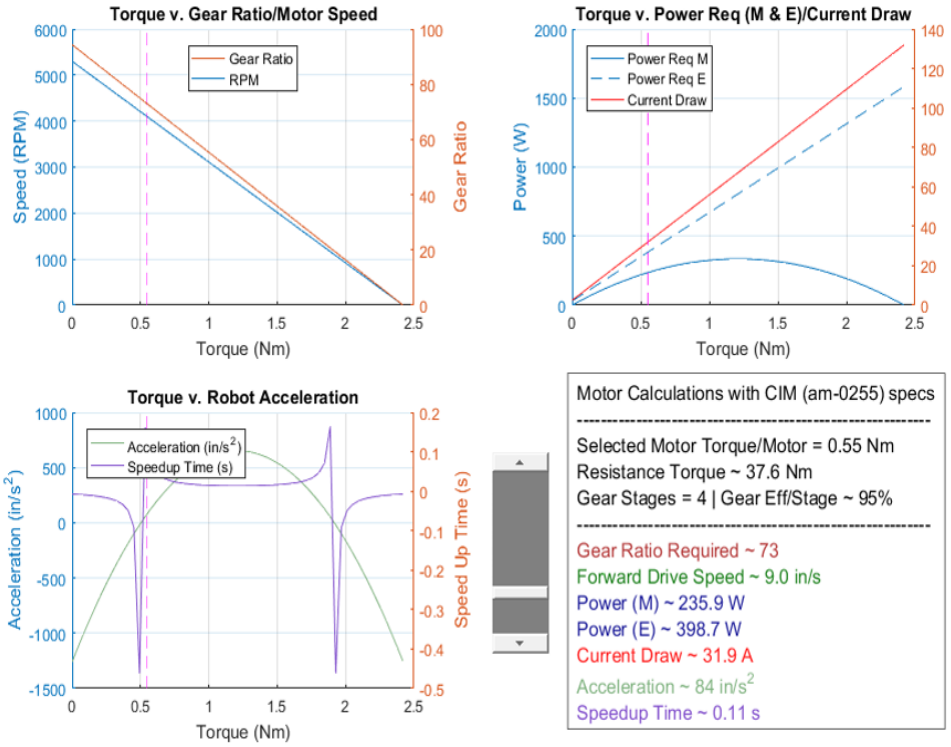

Figure 25: Drive Motor Calculation Curves

3.2 Extraction

The collection system is the core of the robotic mining platform. The collection system is based off of the bucket ladder design[27] but a number of improvements designed to increase rigidity, stability, and to enable mining at 45 cm deep were added.

3.2.1 Scoop Design

The scoops went through many iterations between the prototyping phase and the final manufacturing phase. The scoop teeth in the initial design had a uniform length. It was nearly impossible to penetrate the gravel with this tooth design. In the next design iteration the teeth gradually increased in length towards the center of the scoop. This design efficiently collected gravel as shown in Figures 26-29.

One of the scoop prototypes was made from plastic, which revealed the stress

[27] The bucket ladder design was used by WPI's Moonraker to win the 2009 NASA Lunar Regolith challenge

Figure 26: First scoop prototype

Figure 27: Rocks collected with improved teeth

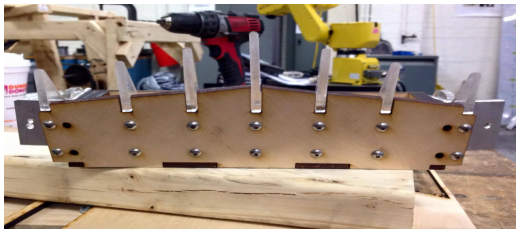

Figure 28: Final scoop prototype

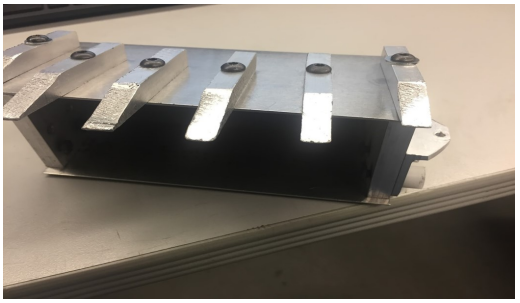

Figure 29: Manufactured scoop

points on the scoops. The plastic teeth often shattered and the connection between the scoop and the chain broke. The final prototype reinforced the chain connection point with aluminum and performed sufficiently to validate the design. The scoop was manufactured from aluminum and tested to confirm that it was sufficiently robust.

3.2.2 Dynamic Chain Actuation System

A traditional bucket ladder system used to dig deep trenches requires a rigid digger to be lowered into the ground. Given the 75 cm height constraint, the digger would need to rotate from a horizontal rest state to a vertical digging state or use a shallow bucket in order to reach the gravel layer 30 cm below the surface. While digging, the deposit height is constantly changing as the mining depth changes. The variable height creates a lot of dust and causes material to be lost before reaching the bucket. These scenarios are illustrated in Figure 30. The Dynamic Chain Actuation System allows for digging from the surface to 40 cm depths with no rotation, constant dump height, and guaranteed material deposit.

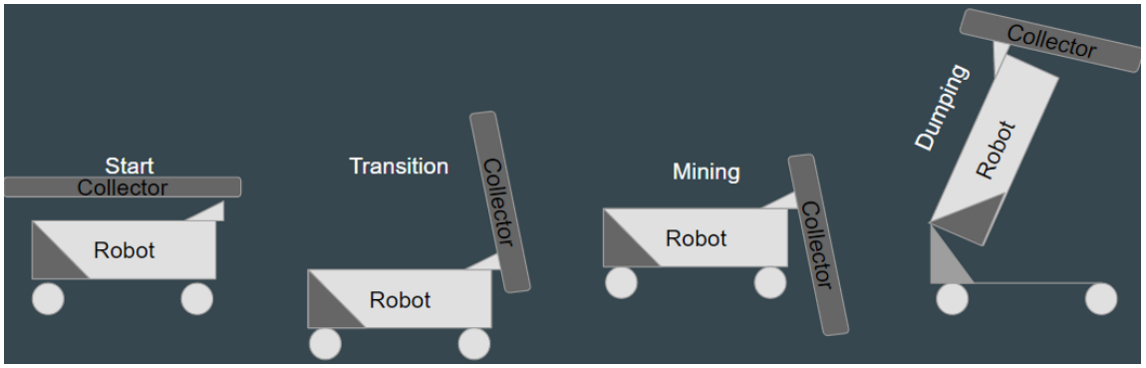

Figure 30: Traditional Bucket Ladder States

Carriage Motion

The system is made up of two carriages: the bottom carriage travels vertically into the ground while the top carriage travels horizontally over the bucket. This is shown in Figure 31. The carriages have a 1-to-1 travel relationship that is controlled using car window regulator tape (dynamic chain). The regulator tape acts as a flexible rack and pinion which simultaneously pushes one carriage and pulls the second carriage with a single motor. This keeps the bucket ladder chain in constant tension as the system changes.

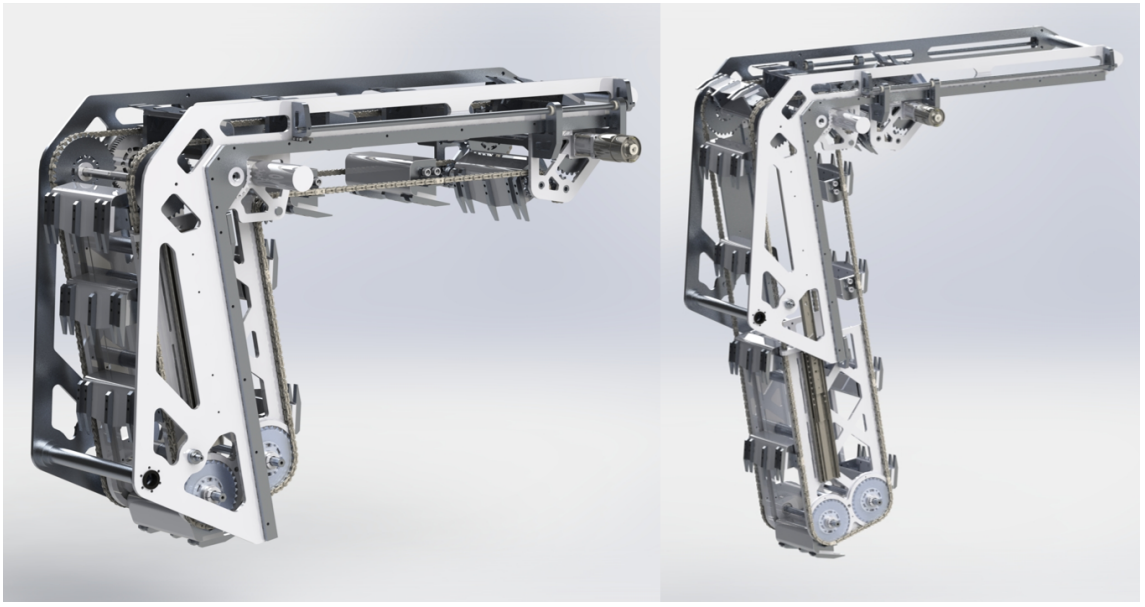

Figure 31: Collector in its retracted and extended positions

Chain and Connection to Scoops

#35 roller chain wraps around the entire system and is driven by two VEX 775pro brushless DC motors, each with a 256:1 planetary gearbox. The chain's movement is independent of the motion of the carriages, allowing the robot to continuously dig deeper into the regolith and gravel. The digging scoops are connected to the chain with tabbed master-links, shown in Figure 32. The tabs allow for scoops to be connected to chain during back-bending, as the sprockets can contact the chain on either side of the link. Another option considered was hollow pin master-links, with the buckets attached to the links using screws. However, hollow pin links are only available for #40 chain or larger, which would have doubled the weight of the system.

Figure 32: Tabbed master link

[28]

[28]https://www.mcmaster.com/#7321k1/=174kuv325

Guide Rail System

The scoop guide rail system located on the lower mining carriage (shown independently in Figure 33) is used to counteract shear forces while digging.

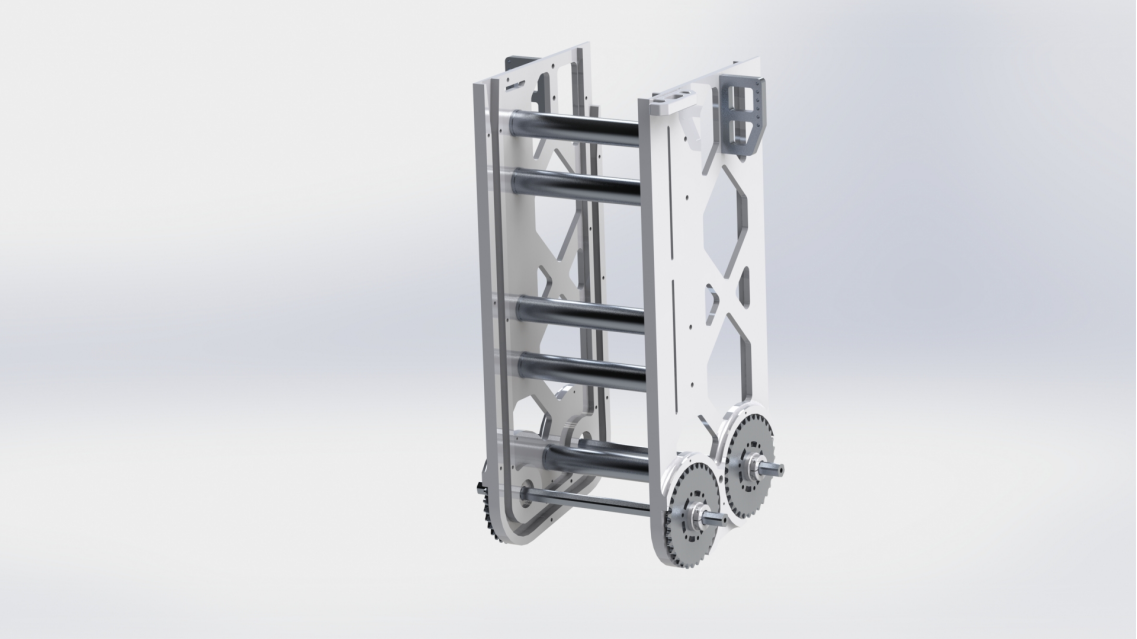

Figure 33: Lower carriage and guide rail system

Each of the scoops has four rollers on it (two on each side) which interlock with a machined slot in the carriage outer plates. The scoops are mounted onto the mining chain via a master link tab on either side of the bucket. These tabs are the weakest link in the system and are prone to tearing under the loads of the regolith mining. The guide rail system solves this by offloading most of the torque from the chain tab onto the guide rails themselves, reducing all the forces acting on the chain to only shear force. Figures 34 and 35 depict free body diagrams of the system both without and with guide rails, respectively.

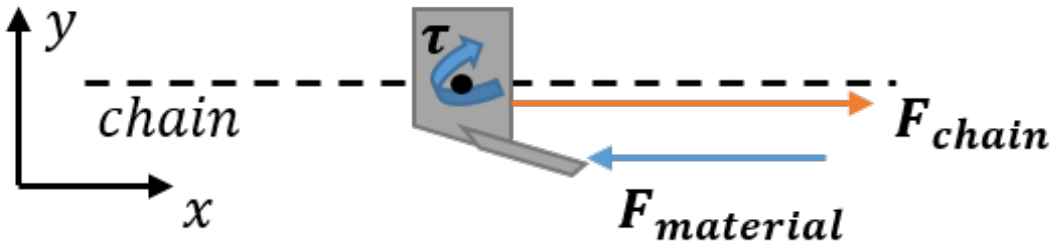

Figure 34: Free Body Diagram for a scoop without guide rails

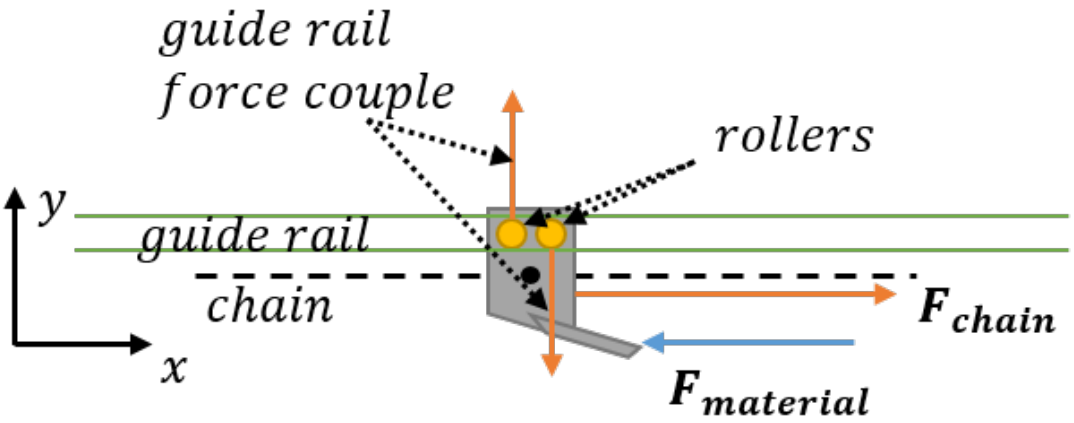

Figure 35: Free Body Diagram for a scoop with guide rails

From these diagrams it is observable that, with the addition of the guide rails, the torque that would have been exerted on the bucket is instead transferred to a force couple on the guide rails.

Figure 36: Entering, disturbing, and pushing gravel

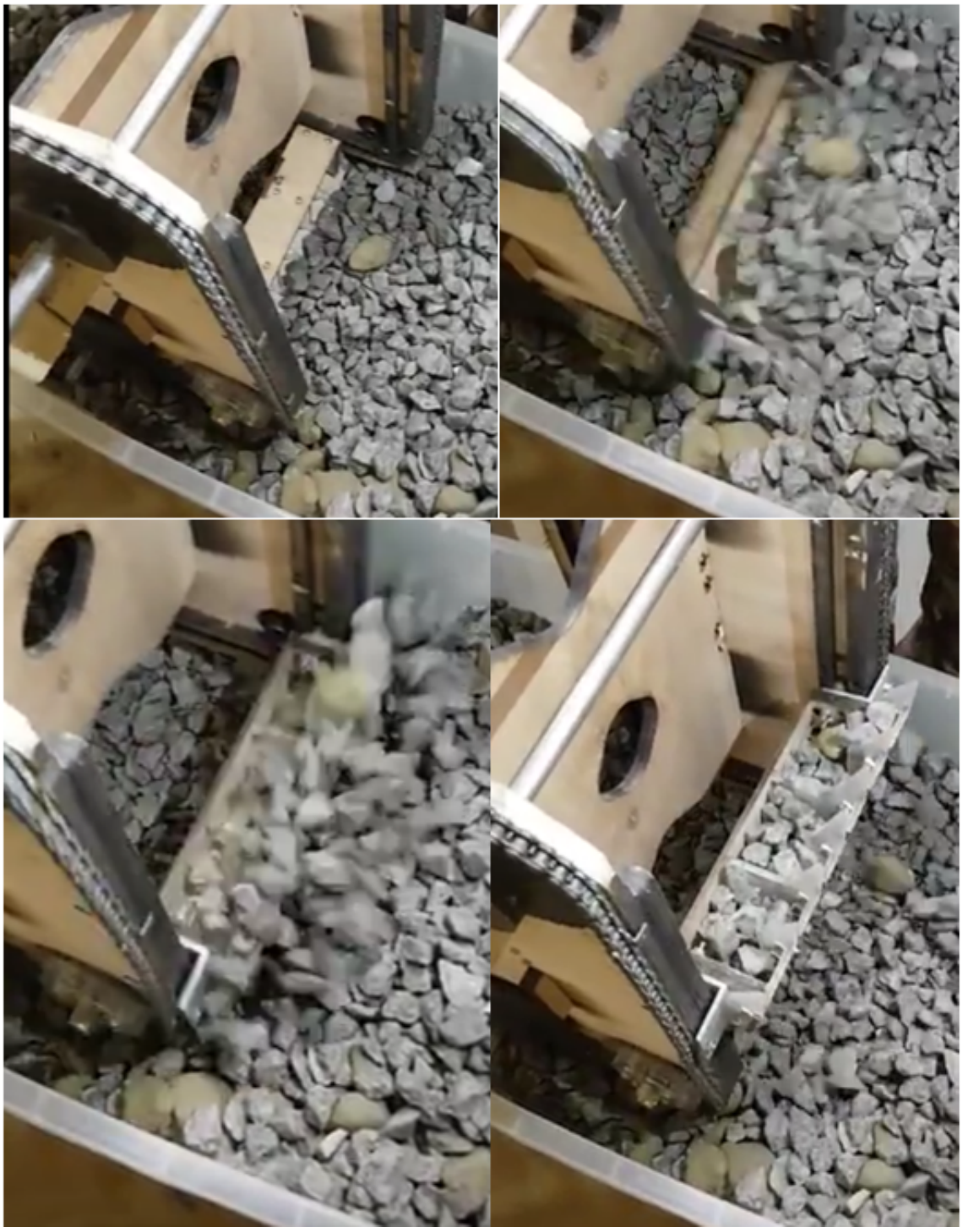

Figure 37: Dig test with double sprocket

Lower Carriage Scoop Path

The initial digger design used one sprocket on either side of the bottom of the digger. Testing in gravel showed that digging in an arc required high torque and resulted in minimal material collection. Breaking the surface of the gravel requires a

motor output of at least 8.5 Nm at 0.305 m/s. This impact generally pushes gravel away from the scoops and causes jamming, which can be seen in Figure 36. The scoop successfully entered and disturbed the gravel, however no gravel entered the scoop. The current design uses two sprockets per side to extend the scoop's path while digging. This allows the scoop to rake in additional material after breaking the surface of the gravel. This is shown in Figure 37 which depicts an early prototype of the collector and scoop breaking the surface, raking through the gravel, and eventually collecting a full bucket of material. Early testing also showed that angles β and θ (Pictured in Figure 38) can affect digging efficiency.

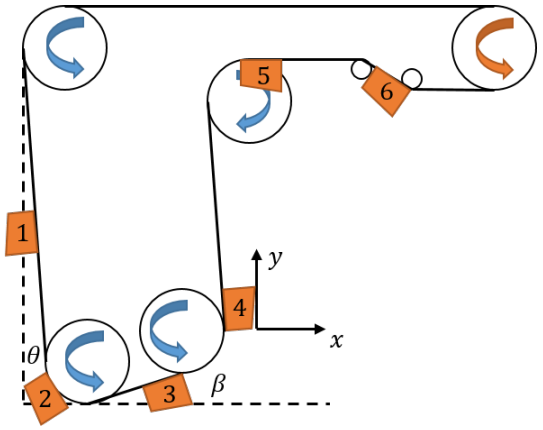

Figure 38: Digging angles

The scoop's angle of attack θ affects how the scoop enters the gravel. An angle of 10 degrees was experimentally determined to be the optimal angle for efficient digging. Angle β is 20 degrees and increases the amount of material collected as the scoop rakes through the gravel. Figure 38 also shows several of the positions that scoops reach during normal operations. Some of the most important of these are position 2, where the scoop first penetrates the material, and 6, where the scoop passes through the two sprockets that cause the collected material to be released into the bucket.

Upper Carriage Scoop Path

Due to BP-1's high repose angle, each scoop is guided through two sprockets to tilt the scoop downwards over the collection bucket. This ensures that all material is dumped into the bucket, and serves to reduce the amount of dust flung by emptied scoops before returning into the ground. These sprockets are shown in Figure 39.

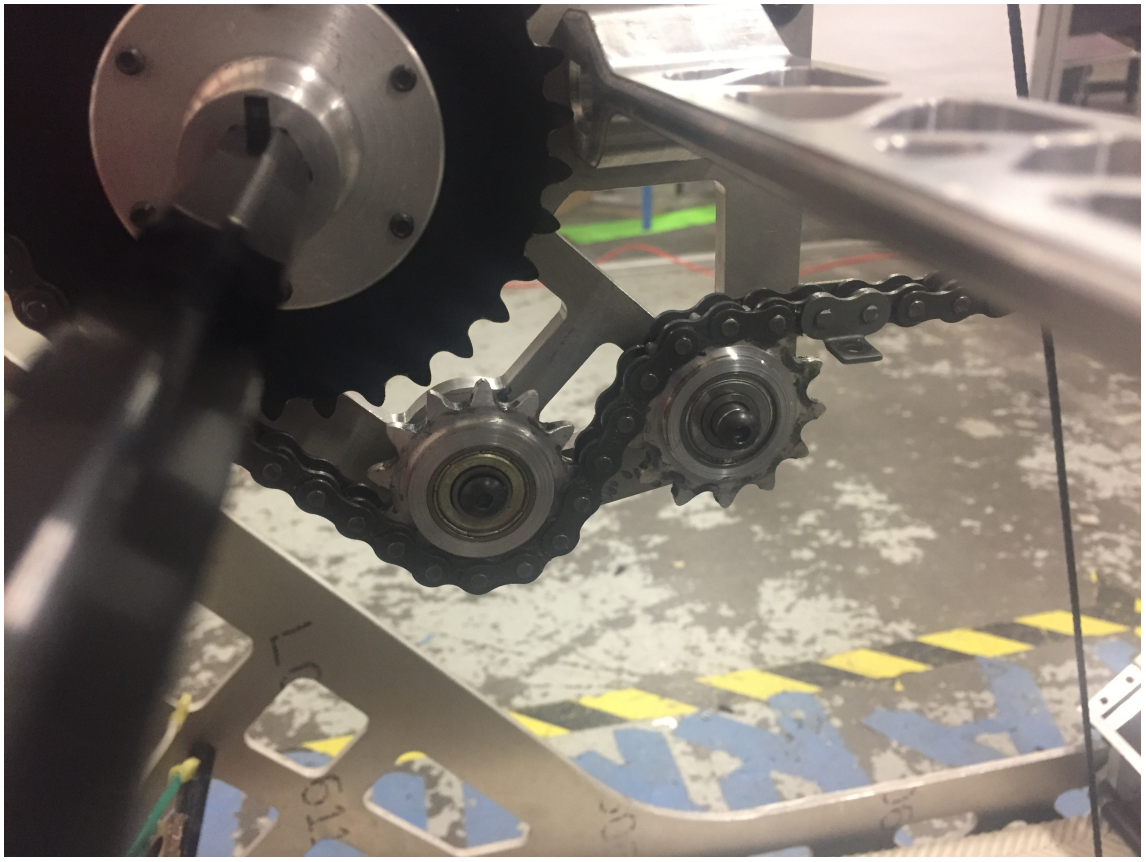

Figure 39: Upper carriage

Digging Motor and Forces

The motor output requirements to dig were determined by driving a digging prototype through gravel with a hand drill. Using the drill clutch to adjust the drill's torque limit, the experimental minimum digging torque was measured at 8.5 Nm. The VEX 775pro motor was selected due to its size, accessible documentation, and availability. Using a BaneBots 256:1 gearbox, the 775pro can output 102.4 Nm and drive the digger at 0.25 m/s.

3.2.3 Manufacturing

The manufacturing for this system involved a combination of many different processes. The structural base is made up of two 1/4 in 6061 aluminum sheets that were cut using a water-jet. The majority of the other components in the system were either turned on a CNC/manual lathe or machined using a CNC mill. Some of the smaller components were 3D printed. The dynamic chain system is made up of a custom milled driving sprocket that interlocks with the car regulator tape. The tape is then housed in aluminum rails to keep the chain rigid.

The lower carriage plates, where the guide rails are located, are machined out of 0.75 in thick 6061 aluminum that is 8 in x 24 in. The rollers are turned on a lathe out of 0.625 in diameter Delrin.

3.3 Material Deposit

3.3.1 Design

The dumping system is designed to deposit a load of 100 kg at a height 0.55 m +/- 0.05 m from the top of the BP-1 surface. To achieve this, the bucket was designed to have a volume capacity of approximately 0.60 m^3, and to rotate about a shaft located at the top of the robot. As the bucket is lifted, the collector is rotated out of the way, preventing collision between the two systems and allowing the extracted material to be deposited. Figure 40 shows the system in the fully raised state.

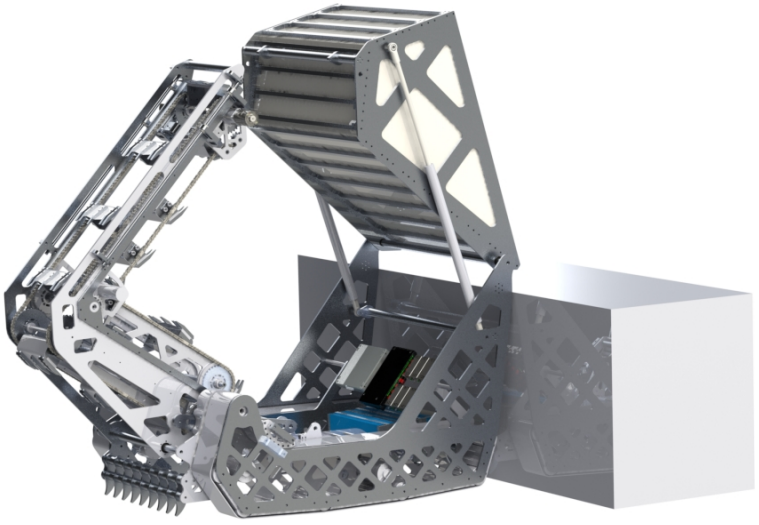

Figure 40: Depositing System

The design revolves around three subsystems: gas spring passive lift, winch retraction, and the synchronization four bar linkage. All three must operate simultaneously to prevent collision between the subsystems.

Gas Spring Passive Lift

A gas spring is a type of linear actuator which relies on stored energy in the form

of built up pressure within a cylinder that moves a piston (shown in Figure 41. The magnitude of the piston's output force is proportional to the pressure inside the cylinder, i.e. as the stroke length increases, the force produced decreases. The force is delivered along the axis that the piston moves in, and is at its maximum when compressed, and at its minimum when extended. Figure 41 shows a diagram displaying generic geometric parameters of a gas spring.

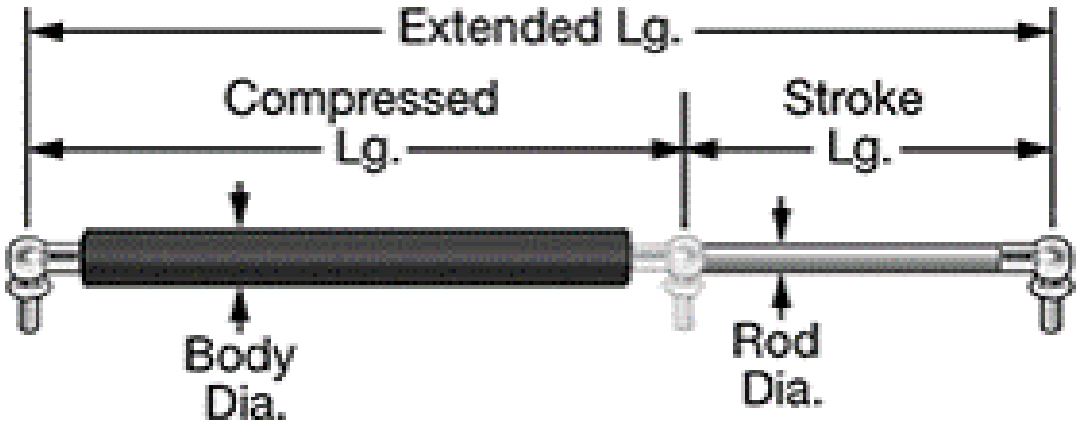

Figure 41: Gas springs diagram

[29]

Each gas shock pivots about two points: its mounting point on the frame of the robot and the mounting point on the bucket. The motion starts at the bucket's resting position and should end when the bucket face (where the material rests) is at an angle 65° relative to the horizontal. At this point, the regolith/gravel mixture's weight should overcome the static friction of the bucket and slide out.

Winch

A winch was selected because it could fully take advantage of the flexibility of where it could attach to the bucket. Since it could be attached on the bucket at a point furthest away from the bucket's rotation point, the winch maximizes the mechanical advantage and minimize the forces acting on the bucket while producing the torque required to perform its tasks.

The winch retracts the bucket after completing the lift while controlling its speed during the process, and actuates the linkage synchronization system. This process depends on the assumption that the cables which connect the winch drums

[29] https://www.mcmaster.com/#gas-springs/=1711f8z

and the bucket are always in tension. If the cable loses tension, then the bucket will not be moving at the same rate as the collector, and thus their positions no longer relate properly to each other.

Since the gas springs are designed to extend relatively slowly, the winch speed must then be constrained to match.

Synchronization Linkage

The last component of the dumping system is the four bar linkage. Since the collection mechanism sits directly over the bucket, it needs to be moved out of the way of the bucket when releasing material. A four bar linkage was designed to achieve the desired motion. This motion is dependent on the winch output shaft, which controls the bucket. In order for the winch to also control the collector, a relationship between the winch output and the four bar crank was calculated to synchronize the two systems. The drive shaft for the crank of the four bar linkage is located on the same shaft as the bucket winch using a custom gearbox. Figure 42 shows a cross-section of the chassis, revealing the winch and linkage setup. The four bar linkage starts in a cross-configuration to rest under the bucket.

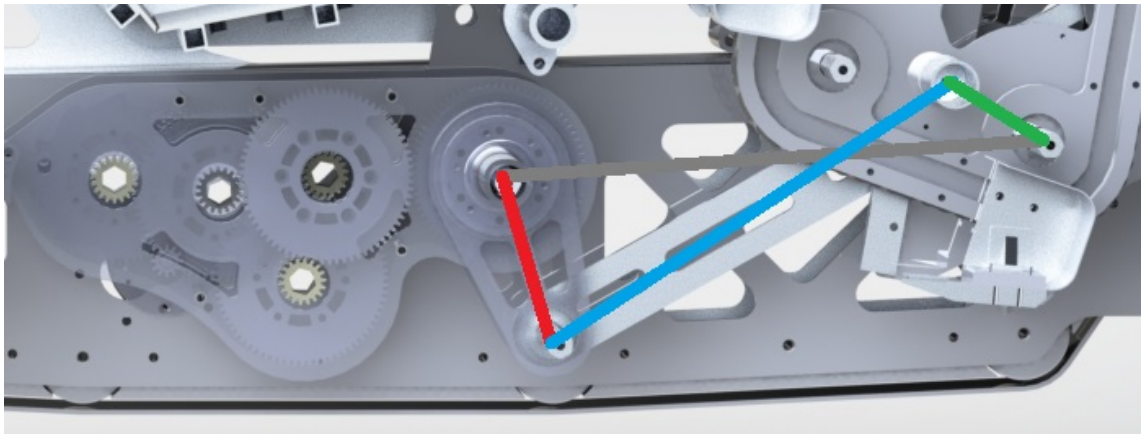

Figure 42: Four Bar Linkage Side View (red:crank, blue:coupler, green:rocker, grey:ground)

The linkage length ratios are as follows: crank: 8.9 cm, coupler: 35.6 cm, rocker: 8 cm, ground: 38.6 cm. The gear ratio required to synchronize the motion is 28:1.

3.3.2 Analysis

Dumping Torque

The actuation of the bucket dumping phase is dependent on two primary factors, T_{cg} (torque payload) and T_{gs} (torque of gas springs). In order for the system to

perform the operation, the following condition must hold true: $T_{gs} > T_{cg}$. Since the torques vary with respect to the position of the bucket, q (sliding face in degrees relative to vertical), calculations were performed from the starting position (48°) to the target position (155°) to ensure that the following condition is met at all points from start to finish.

$$T_{gs} > T_{cg} \tag{1}$$

Figure 43 shows the three major forces acting on the bucket relative to the bucket rotation point O.

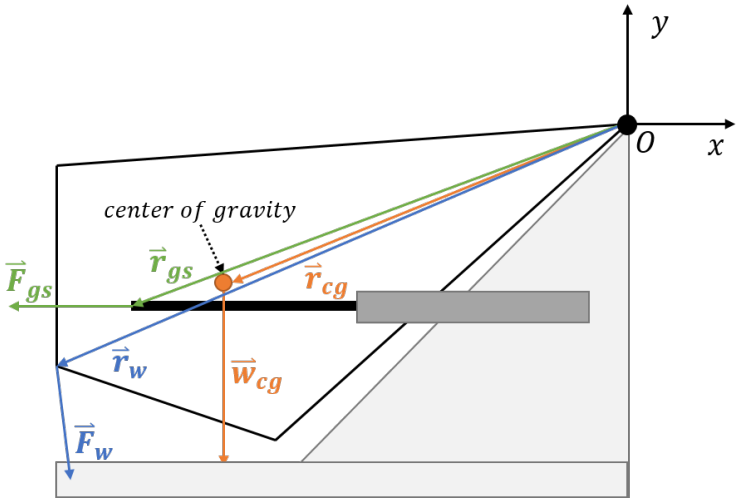

Figure 43: Bucket Force Diagram

Using the Equation 1 and Figure 43, the following equation was derived:

$$\|\vec{r}_{gs} \times \vec{F}_{gs}\| > \|\vec{r}_{cg} \times \vec{W}_{cg}\| \tag{2}$$

Each variable in Equation 2 is either known or can be approximated. This model was implemented in MATLAB, which performed the calculations over the range of possible bucket angles to ensure that the inequality holds true. Figure 44 shows the torque curves for the gas springs and the payload.

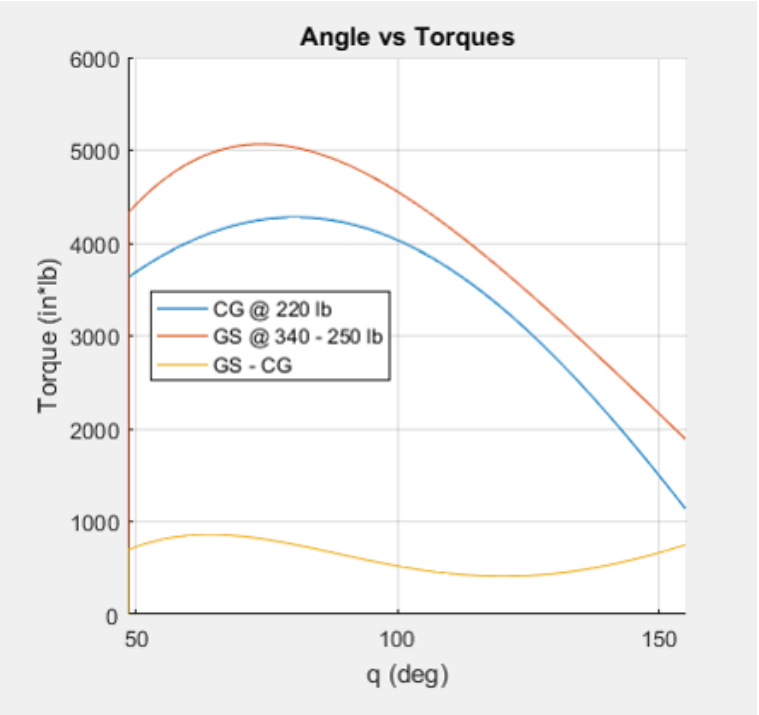

Figure 44: Angle vs Torque Curves Dumping Analysis

In order to lift 100 kg (∼220 lbs) including the mass of the bucket itself, two gas springs with a rating of 1.51 kN (∼340 lbs) compressed and 1.11 kN (∼250 lbs) extended were selected. These values were used in the torque calculations. In the figure above, the gas spring curve (orange) encloses the payload curve (blue), which guarantees that at every point over the course of the dump the difference curve (yellow) is always positive. The positive net torque means that the bucket will always be trying to lift.

Winch Requirements

Using the data generated from the bucket torque curves, the force exerted by the winch is obtained. Figure 45 shows winch data over the course of the dump. The winch drum has a 2 in diameter, thus the moment arm of the drum is 1 in. The maximum value of the winch force curve is 82 kg (∼181 lbs), which means that this value is the minimum value that the motor and gear ratio should be designed for. The gas springs' torque curve was used to generate this curve because the resistance torque on the winch is the highest when there is no material in the bucket, thus T_{cg} = 0. The following condition must be satisfied to ensure retraction:

$$T_w > T_{gs} \tag{3}$$

$$F_w = \frac{T_{gs}}{R_{wdrum}} \tag{4}$$

Figure 45: Winch Force Curve

Figure 46 shows the results of these equations as the winch rotates. Using the obtained value for the winch, motor calculations were performed to satisfy the constraints. The chart shows the ideal case results. However, the particular numbers may not be feasible to achieve. For instance, 103:1 is most reasonably approximated to 100:1 and will achieve a slightly less optimal effect. In addition to the ideal calculations, inefficiencies must also be considered during the calculations. Gear inefficiency has been approximated to 5% per stage, and a 20% safety factor has been added to account for other inefficiencies such as friction, dust, and other factors. The goal was to find an appropriate gear ratio that minimizes the current draw and total retraction time while being able to satisfy the force requirement. Given the motor's 0.46 Nm output torque, a 100:1 gear ratio is required to achieve the necessary output torque. Note: 136 kg (∼300 lbs) was used as the desired winch force, although 82 kg (∼181 lbs) was the calculated requirement. The reasoning behind this decision is because the gas springs could easily be replaced with stronger ones of the same dimensions allowing the system to dump a larger load. There is little disadvantage in allowing a higher gear ratio (trading an insignificant amount of extra time to dump in exchange for the potential to dump more after optimization through testing).

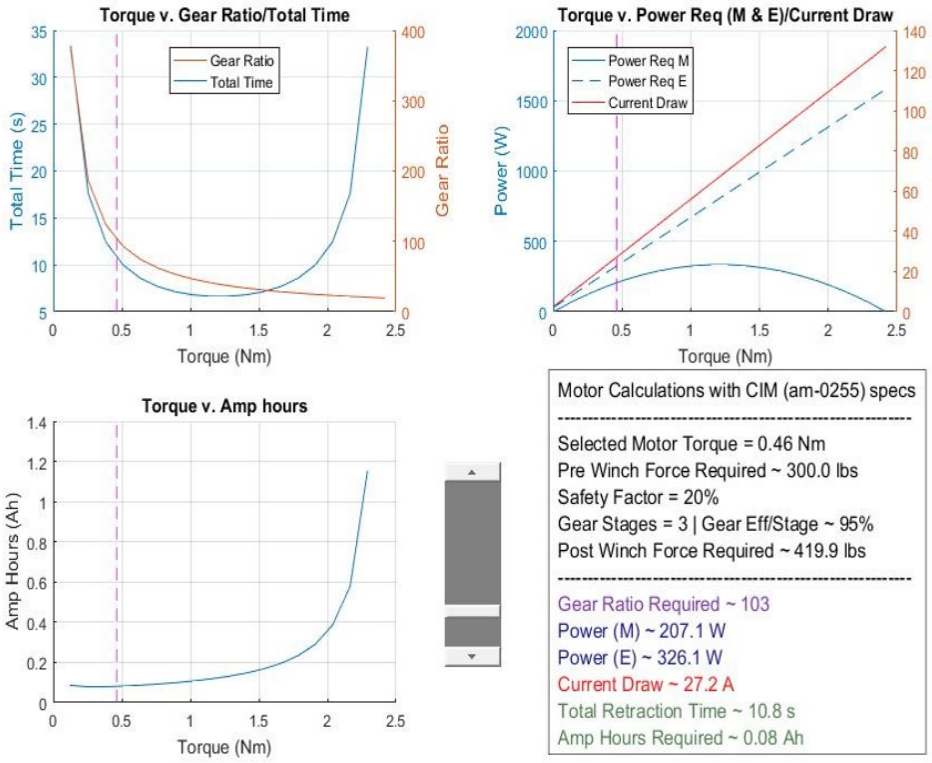

Figure 46: Winch Motor Calculation Curves

Four Bar Linkage

The simplest calculation for a four bar linkage is the Grashof Condition, which is shown by Equation 5. By applying this inequality, several important properties of the four bar are obtained: 1) whether there is an instability point and 2) whether the crank can perform a full rotation under the constraints of the rest of the links.
Grashof's Law

$$S + L < P + Q \tag{5}$$

Let: 'S' = length of shortest link,
'L' = length of longest link,
'P' = length of either of the two other links
'Q' = length of remaining link.

When this inequality is applied to the design, the result is the following:

$$Crank + Ground < Rocker + Coupler$$
$$8.9cm + 38.6cm < 35.6cm + 8cm$$
$$47.5cm < 43.6cm$$

Clearly the inequality is **false**, which by Grashof's Law implies that the four bar crank cannot perform a full rotation. It also implies that there should not be an instability point, which would have been the case if the following condition was met.

$$S + L = P + Q$$

From a controls perspective, what this means is that caution should be taken when actuating the winch motor in order to avoid rotating past the extreme end positions of the four bar. Since the instability condition was not met (for the purposes of the robot, the mechanism will never attempt to enter an impossible position), the four bar should never encounter a situation where its behavior is ambiguous, which increases the robustness of the system.

Ideally, the system should also meet the Grashof condition to avoid failure cases. However, due to geometric constraints, it was not possible to achieve the desired motion while meeting the Grashof condition. Other candidate solutions physically interfered with the other subsystems. This solution satisfied the objective of clearing the bucket while fitting within the size restrictions for the robot.

Using *Linkages Student Edition* software, the parameters of the four bar linkage were used to generate SVA charts. One of the main objectives was to analyze the velocity curves to find the maximum speeds that the four bar rocker will be traveling at. The rocker is connected to the collector which means that the collector will be moving at a speed proportional to the rocker. Figure 47 shows the velocity and acceleration curves of the point joining the rocker and the coupler links (I 3,4).

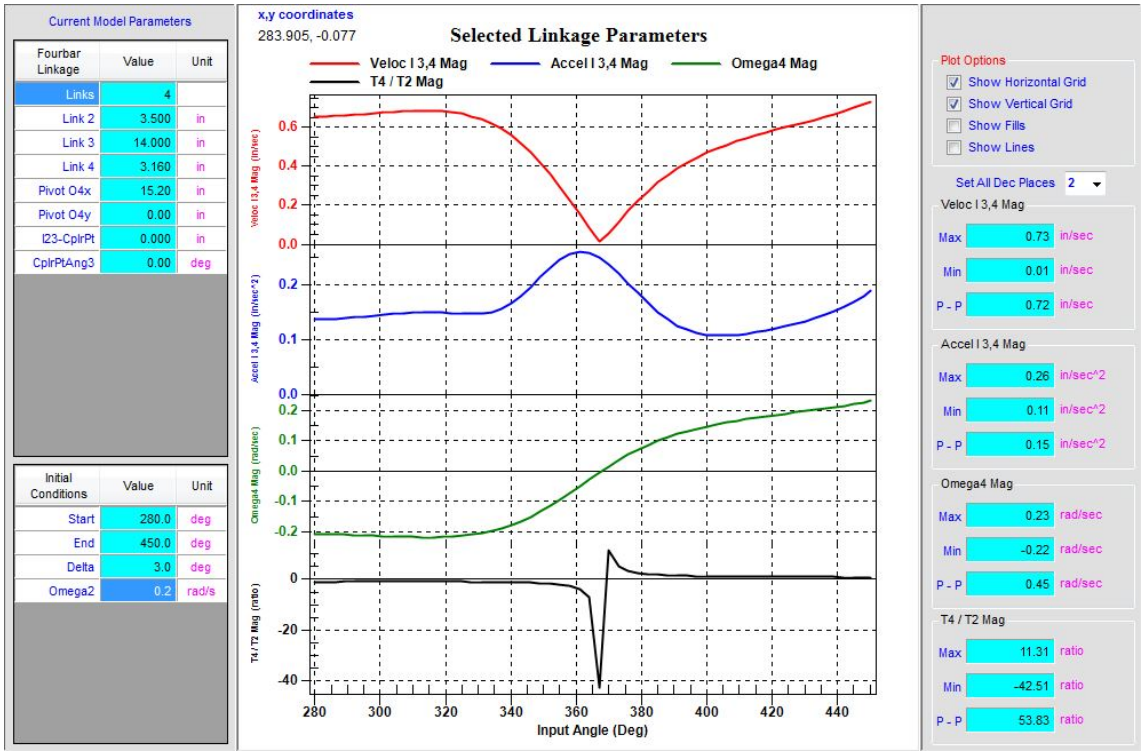

Figure 47: Four Bar Velocity Acceleration and Torque Ratio Curves

The link lengths were inputted (in imperial units) along with an estimate of the angular velocity, ω_2, of the input link into *Linkages Student Edition*. The input, ω_2, was calculated by simply applying the gear reduction from the CIM motor actuating the winch to the crank of the four bar linkage (280:1), assuming no load on the motor. The result is approximately 0.19 rad/s. The upper red curve shows the magnitude of the velocity of (I 3,4). It is clear that the local maxima occur near the start and end of the motion of the four bar linkage. The point at which the velocity drops to 0 in/s indicates the rocker's change in direction.

The extrema are listed for each chart on the right. For the velocity magnitude curve, the maximum speed of the rocker peaked at 0.73 in/s. This implies that perhaps the speed of the motor may need to be reduced towards the beginning and end of the cycle in order to avoid instability due to the momentum of the collector. It also means that running the motor at higher speeds midway through the cycle would be reasonable.

System Synchronization

After selecting configurations for the bucket lift and the collector four bar linkage, the final step was to derive the relationship between the winch output and the crank of the four bar linkage. This was achieved by assuming an angular velocity of the

bucket, ω_b, and experimenting with values for the four bar crank ω_c relative to ω_b in order to find solution candidates in a MATLAB simulation. These candidates needed to satisfy the clearance constraint to avoid collision between the collector and the bucket while satisfying the initial condition of the start position. The angular velocity of the winch output, ω_w, was estimated by approximating the rate at which the length of the winch cable changed. Using the result of this calculation, ω_w can be approximated and a relationship can be found between ω_b and ω_w. Using this value and the relationship between ω_b and ω_c, the ratio between ω_w and ω_c comes out to be 28:1. Figure 48 shows various orientations of the collector as the bucket is raised.

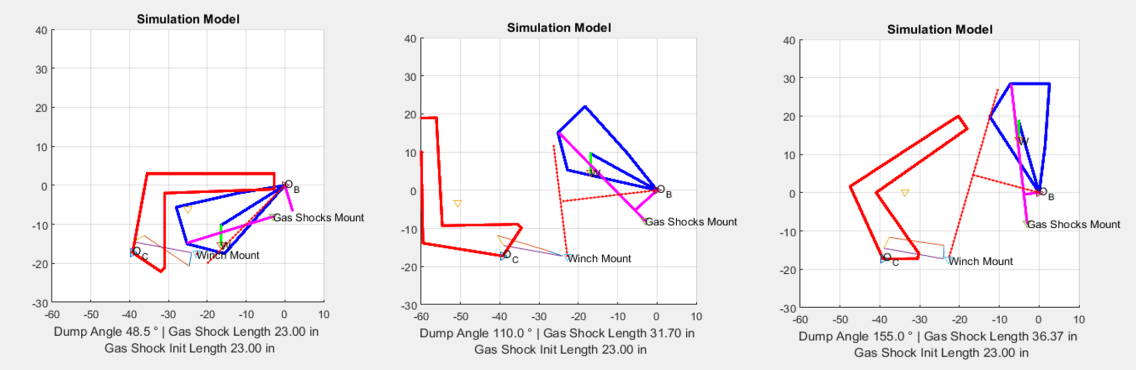

Figure 48: Simulation Model Form Conversion

4 Control System

4.1 Electrical Structure

The electrical system for Markhor consists of 4 main systems:

- Power
- Motor Control
- Sensor Control
- Main CPU

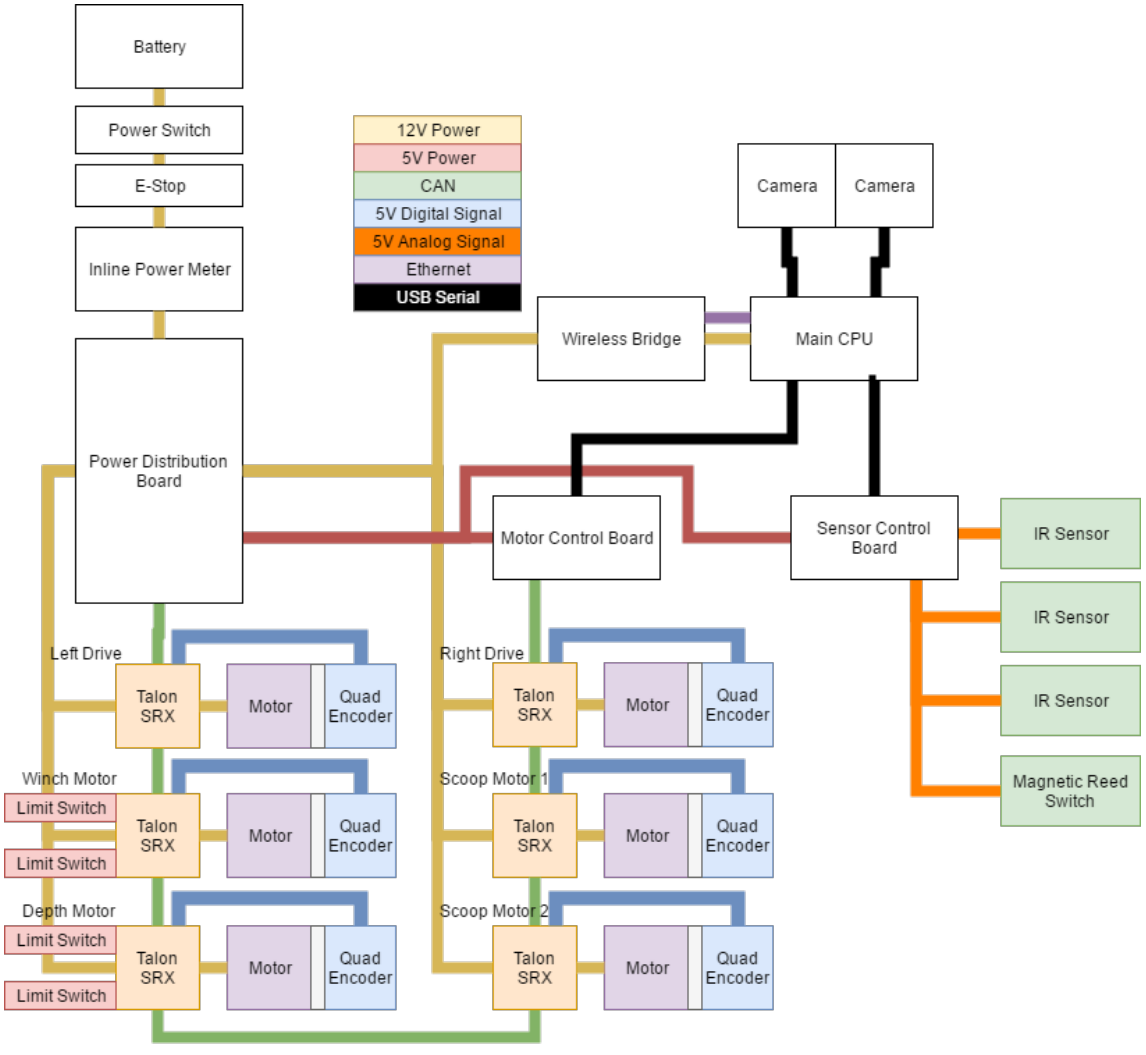

Figure 49: Electrical Systems Diagram

4.1.1 Power Distribution

The main power source for the robot is a 12 V, 18 Ah lithium ion battery. The battery is connected in series with a power switch and an emergency stop relay; pressing either of these switches will immediately cut power to the entire robot. The switches lead to an inline power meter, which measures the total power consumed by the robot as it operates. Finally, the 12 V supply enters the Cross the Roads Electronics (CTRE) Power Distribution Panel, which provides regulated supplies to the rest of the on-system electronics.

4.1.2 On Board CPU

The main processing unit is a Fanless Compact Embedded MicroBox PC from SuperLogics (Figure 50) which interfaces with the Motor Control Board (MCB), Sensor Control Board (SCB), and the cameras.

Figure 50: MicroBox PC from SuperLogics

This device was selected because it offers many of the benefits of a standard laptop computer while maintaining a rugged and compact form. The MicroBox connects with the wireless bridge in order to receive commands and send sensor data to the Control Station Computer (CSC). The CSC is a standard laptop running a custom Java application.

4.1.3 Motor Control

All motors are driven by CTRE Talon SRXs. These motor controllers were selected for a variety of reasons. A primary motivation for using them is that each Talon SRX can directly read the inputs of encoders and limit switches, allowing them

to perform closed loop feedback control. Instead of having to perform six PID loops on the main processing computer, each loop is instead calculated automatically by its corresponding Talon SRX. All of the Talon SRXs are connected to the same CAN bus, which allows status and control messages to be rapidly propagated between the devices. The Talon SRXs interface with a HERO Development Board (Figure 51) which functions as the Motor Control Board (MCB) for the robot. This board also natively supports CAN and has a custom API that allows for easy control of the Talon SRXs. The MCB is connected to the Robot Controller with a TTL-to-USB adapter.

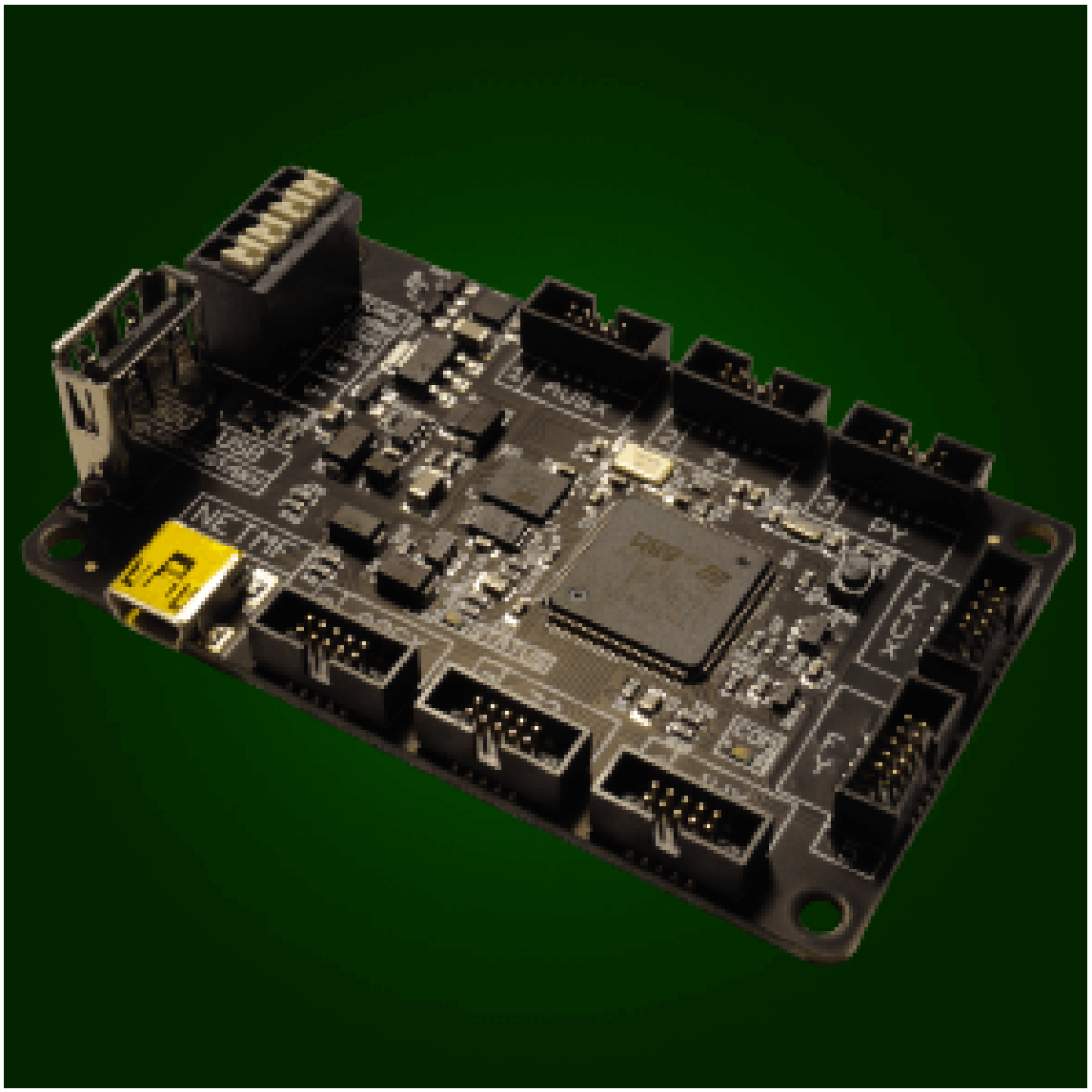

Figure 51: HERO Development Board from Cross the Road Electronics

4.1.4 Sensor Control

The Sensor Control Board (SCB) is an Arduino Mega. The SCB is used to control the feedback from the Sharp Infrared (IR) Proximity sensors that are used to detect material in the dumping bucket. The IR sensors were chosen for material collection because they can be used to detect variable changes in distance, allowing an estimate of the amount of material in the dumping bucket to be made. The SCB also monitors a Magnetic Reed Switch that is used to check scoop positioning during material collection.

4.2 Software Control

The software control system for Markhor relies on four systems continually communicating and exchanging data. These systems are:

- The Motor Control Board,
- Sensor Control Board,
- The Control Station Computer, and
- The Robot Controller

Figure 52 outlines the high level communication structure of the software control system.

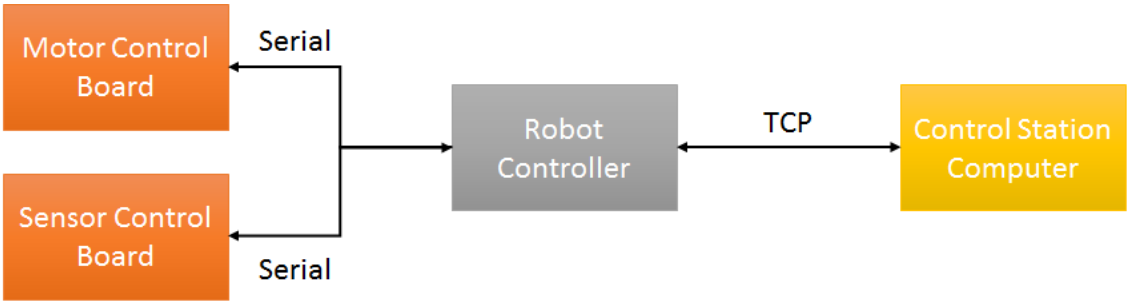

Figure 52: Communication between the four different parts of the software control system

4.2.1 Motor Control Board

In order to interface with the Talon SRX motor controllers, the HERO Development board was chosen as the Motor Control Board (MCB). Both the Talons and HERO are manufactured by Cross The Road Electronics, and the HERO includes a C# API specifically for communicating with the Talon SRXs.

The MCB communicates over a 115200 baud serial connection with the robot controller. The MCB accepts messages in the following ASCII format:

<DEV_ID:MODE:SETPOINT>

Multiple messages can be sent at once; the end of a message stream is denoted with a newline character. As these messages arrive, the device ID is checked against the set of valid device IDs. If no match is found, the message is dropped. If there is a match, the Talon SRX with the corresponding device ID has its mode and setpoint updated according to the information provided in the message.

The Talon SRXs maintain a large amount of information about the motor they are controlling. Values of particular interest are the speed and position of the motor, the current through the motor, the status of the motor's limit switches (for the collection system/bucket system), and more. The MCB assembles these messages in the following format:

<DEV_ID:CURRENT:TEMP:VOLTAGE:SPEED:POSITION:
SETPOINT:MODE:FWD_LIM:REV_LIM>

These messages are then sent back to the robot controller. The goal of this system is to essentially act as a hidden 'middle man' that allows the Robot Controller to seemingly communicate directly with the Talon SRXs.

4.2.2 Sensor Control Board

The Sensor Control Board (SCB) functions very similarly to the MCB. The SCB also communicates over a 115200 baud serial port with the robot controller. Unlike the MCB, the SCB does not receive messages from the robot controller. Instead, it only pushes information to the robot controller. Each message from the SCB takes the form:

<SENSOR_NAME:VALUE>

The robot controller processes these messages by checking the sensor name against the names of all the sensors defined in the system. If the sensor name matches, the value associated with that sensor is updated on the robot controller. As with the MCB, the SCB is designed to provide an invisible interface between the robot controller and the sensors themselves, such that software on the robot controller can essentially access the sensors directly.

4.2.3 Control Station Computer

The control station computer (CSC) is a user application that runs a Java GUI. It is designed to allow an operator to easily interact with the robot. The three primary functions of the CSC are to maintain a queue of actions for the robot to execute, display information received from the robot, and provide a formatted stream of communication between the operators and the robot. Figure 53 shows a UML diagram that depicts the general outline of the CSC.

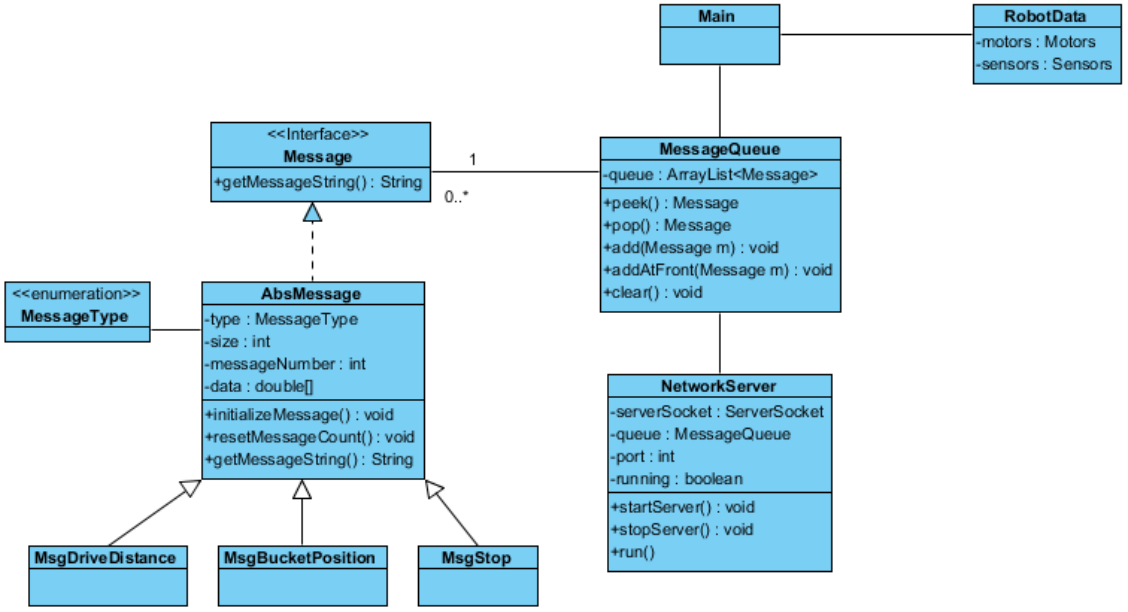

Figure 53: UML diagram depicting the structure of the CSC

All of the commands the robot should execute are maintained in a queue (MessageQueue). The MessageQueue functions as a priority queue that allows items to be typically added in a first in, first out fashion, but also allows new commands to be added to particular positions within the queue. This serves the dual function of allowing the operator to modify the robot's execution path at runtime by adding or removing operations, and also allows emergency stop commands to be immediately added to the front of the queue. In a typical usage, the queue would be populated with all the commands needed to complete a ten minute mining operation autonomously. In the event the robot incorrectly performs one of the commands in the queue, a new command can easily be added to get the robot back on course.

Each message in the MessageQueue implements the Message interface and contains 3 key elements: the type, the number, and the associated data array. The message type is an enumeration that determines how the message data should be processed. The message number is used by the robot controller to determine when

a new message has arrived (if two identical messages are sent in sequence, some method is needed to determine when the first task has completed).

The CSC acts as a TCP server that responds to requests from the robot controller (which acts as a TCP client). Each request from the robot contains the most recent set of motor and sensor values to be displayed on the GUI. Each request response is populated with the Message at the front of the Message Queue and returned to the robot controller. Upon receiving the Message, the robot controller can interpret and act accordingly. This format allows for minimal data bandwidth between the robot and the CSC, as messages are only required to be sent when a command finishes. This is important because communication bandwidth with a rover deployed on Mars would be assumed to be minimal. Figure 54 shows a screenshot of the GUI's basic setup.

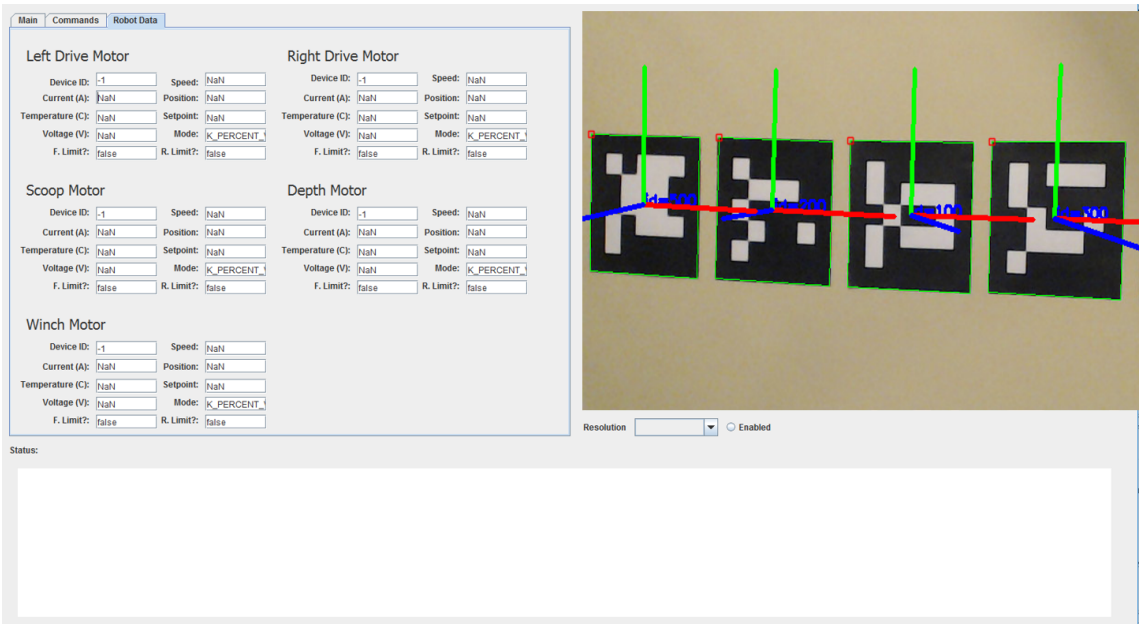

Figure 54: Screen capture of the Control Station GUI

4.2.4 Robot Controller

The robot controller is the core control system for the robot and is responsible for sending messages to all of the other subsystems. Figure 55 shows a UML diagram explaining the classes that comprise the robot controller.

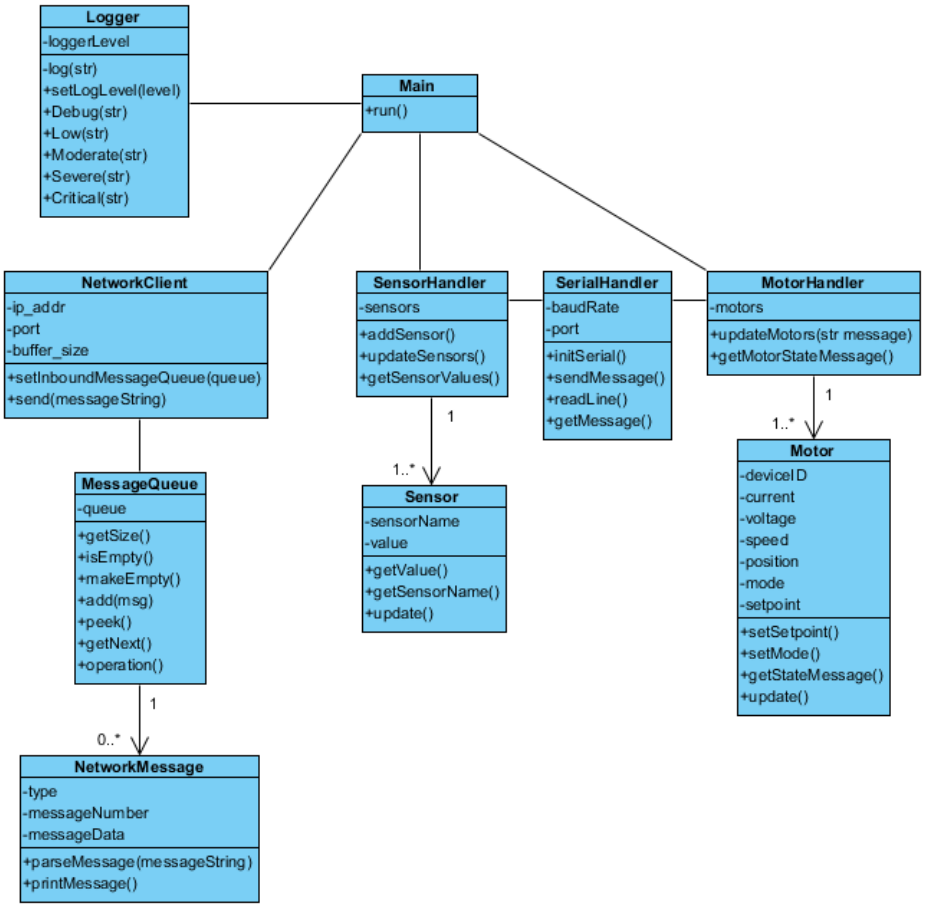

Figure 55: UML diagram depicting the classes comprising the Robot Controller

The SerialHandlers are responsible for processing reads and writes from their associated boards. Because the serial communications are running constantly, each SerialHandler runs within a thread that loops continuously.

In addition to the two serial communication threads, the robot controller also runs a main loop where a majority of the robot's actions take place. Figure 56 depicts a flowchart of each execution of the main loop.

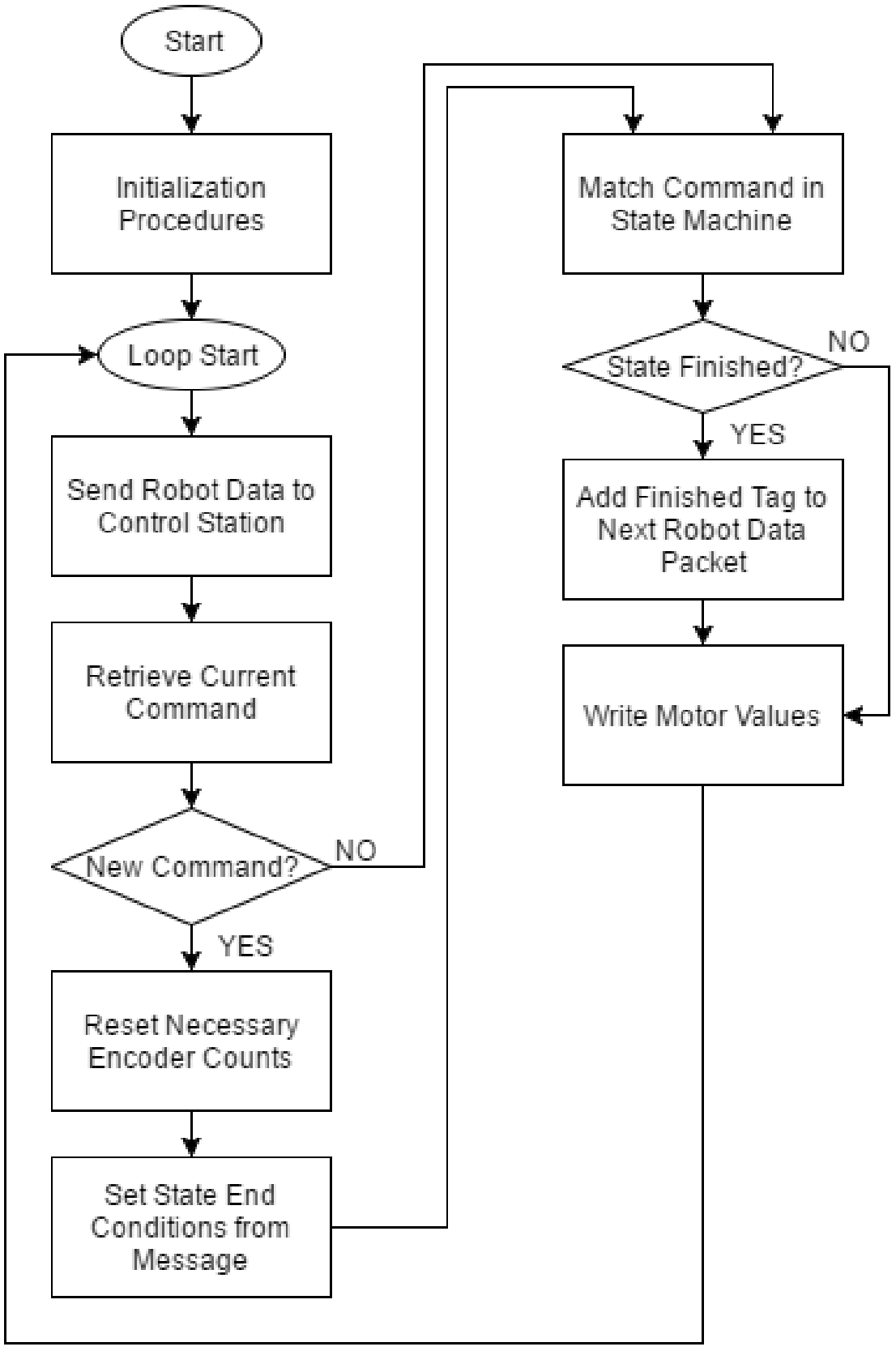

Figure 56: UML diagram depicting the classes comprising the Robot Controller

The loop begins by having the robot push all of the relevant motor and sensor data to the CSC so that it can be displayed in the GUI. In the TCP response to this message, the robot controller receives a message indicating the command it should be executing. The proper motor values to be written are selected with a switch statement. Each switch case also constantly checks if the end conditions for the current state have been met. If so, the robot controller notifies the CSC and requests the next command in the MessageQueue. Finally, the loop delays to maintain a constant 10ms execution time for each iteration of the loop.

5 Performance Evaluation

5.1 Locomotion Evaluation

5.1.1 Driving Straight

To evaluate the robot's speed, it was placed in a sand pit and driven in a straight line. The robot was able to travel 1.524 m (5 ft) in 5.80 s, yielding an approximate drive speed of 0.262 m/s (10.3 in/s). The current through the drive motors was monitored during this period and is shown in Figure 57.

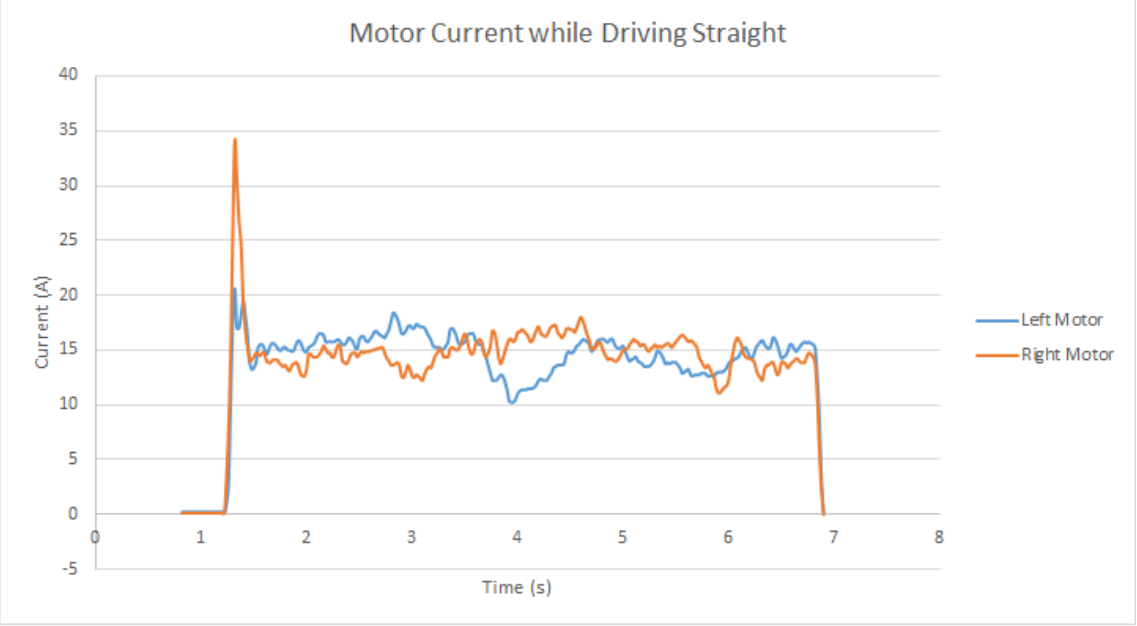

Figure 57: Current in the left and right drive motors while driving straight

The current peaks for both motors as they move from being idle to running, with the left motor seeing a peak of 34.1 A. The current then normalizes to an average of 14.65 A per motor until the robot stops. Given that the robot uses a 12 V battery, the drive system consumes 352 W. Assuming the robot spends two of the ten minutes of runtime driving, it would use 0.977 Ah (5.42% of the battery's capacity).

5.1.2 Rotating

The robot's turning speed was evaluated similarly to its linear speed. After being placed in the sand pit, the robot was able to turn 180° in 4.92 s, yielding a rotation speed of 36.6°/s. The current while turning was also measured and is shown

in Figure 58. Excessive turning was observed to cause the left tank tread to become misaligned from the self guided track. The two main culprits were determined to be low belt tension, and lack of a Delrin block on the front upright portions of the track. In the worst case scenario the belt can be realigned by turning in the opposite direction. Additionally, the issue was resolved after re-tensioning the left tread. A Delrin block on the upright portion of the tread might be added prior to the RMC depending on weight, and material availability.

5.2 Obstacles

The robot was able to successfully push a 20 kg rock sitting on the surface of the sand pit that was blocking its path [Figure 60]. During further testing with the rock partially submerged the robot was unable to move it. For reference, the largest rock that could be encountered during the RMC will be only 10 kg. The robot was tested driving through two different craters, the first was 30 cm deep by 30 cm in diameter. The robot drove over the crater with no problems. The robot was also tested driving through a larger crater 30 cm deep by 60 cm wide. The robot succeeded in driving straight through the crater and reversing through the crater as can be seen in Figure 59. The robot also succeeded in driving through the crater with one track module in the crater, and one module outside the crater. However the robot got stuck while reversing through the crater. Initially the robot could re-exit the crater driving forward, however after multiple attempts to reverse out of the crater the robot was completely stuck.

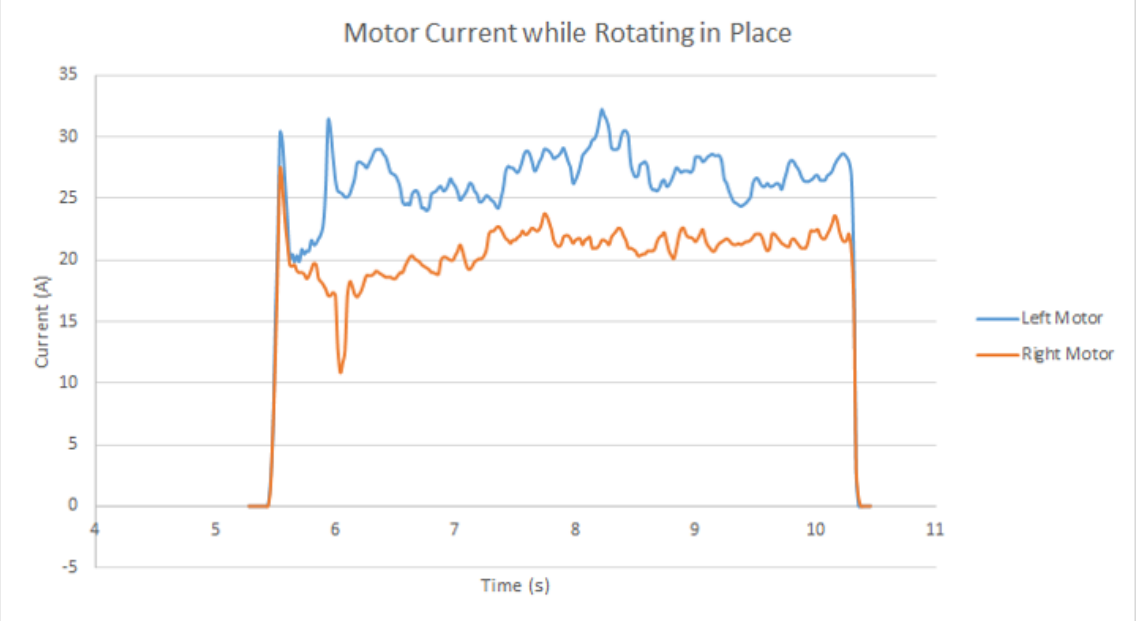

Figure 58: Current in the left and right drive motors while rotating in place

Rotating in place requires, on average, 46.4 A across both motors. Rotating requires 557 W, which is significantly more than driving linearly. Assuming the robot spends one minute rotating, it would use 0.773 Ah (4.29%).

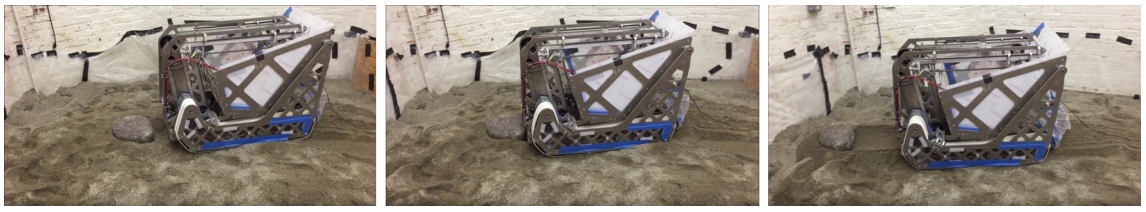

Figure 59: Robot pushing 20 kg rock

Figure 60: Robot driving through large crater

5.3 Collection Evaluation

At the time of writing, the collection system was evaluated with a single scoop. This was in part due to not having yet manufactured the remaining scoops, but also allowed for a full analysis of the scoop's travel through the system.

Despite having only one scoop the collector successfully dug a hole to its maximum depth of 40.6 cm (16 in) collecting both sand and gravel. As expected the sand caused no problems during collection. The initial scoops through the gravel were also successful. However as the collector continued to collect scoops of gravel the chain began to pop off the sprockets. This occurred because rocks would fall between the chain and sprocket at the bottom of the carriage. This was solved by adding a protective sprocket as seen in Figure 63. This additional sprocket pushed rocks away from the chain and restricted any sideways motion of the chain, should it slip off the teeth. The material collected during the test can be seen in Figure 62.

Figure 61: Collection of sand and gravel

Figure 62: Sand and gravel collected by scoop

Figure 63: Outer Sprocket to prevent chain slip

5.3.1 Collecting Sand and Regolith

Because of its limited availability, testing with BP-1 was impossible; sand was used as a stand-in, as it has similar properties to Martian regolith. Figure 64 shows the current in both of the scoop motors as the scoop traveled through the sand.

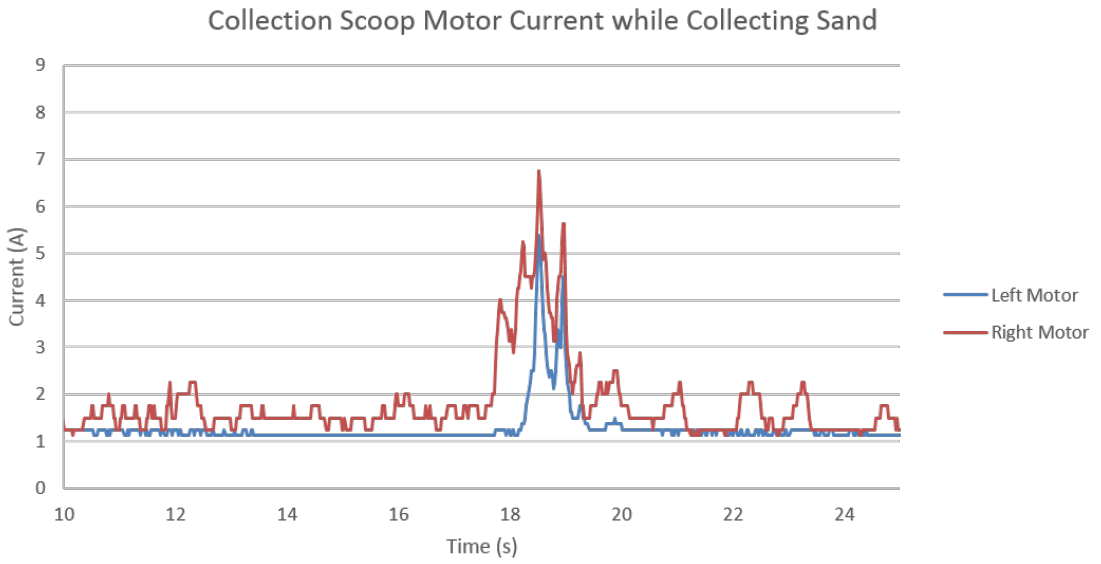

Figure 64: Current in the left and right scoop motors while collecting sand

While the scoop was not submerged in the sand, the system drew very little current; on average each motor used between 1.0-1.5 A. When the scoop entered the sand (around the 18 second mark in Figure 64), the current in each motor only peaked briefly to 6.5 A before dropping back to the lower "idle" current. When completely full, each scoop holds approximately 0.91 kg of sand. An interesting point to note is that even as the scoop of sand was lifted (around the 20 second mark), the current required to lift the sand was no more than the idle current. Because of the 256:1 gearing on the scoop motors, the full bucket of sand had a negligible impact on the power required to operate the system.

The average current through the system (including the scooping time and idle time) was approximately 3.24 A. Therefore, scooping sand with a single scoop requires only 38.9 W; this number would be expected to increase with the addition of more scoops. However, even assuming a worst case of 14.625 A continuously (a sum of the highest currents experienced by each motor), the total power draw would only be 176 W, which is less than half of the power required for driving straight. Assuming the robot spends 5 minutes collecting sand or regolith, only 1.22 Ah would be used in the worst case scenario (6.78% of the battery's capacity).

5.3.2 Collecting Gravel and Ice

Ice chunks are logistically difficult to test with, so pieces of gravel with a mean particle size of 2 cm were used. The same procedure for testing the collection of

sand was applied to the collection of gravel: Figure 65 shows the current through the scoop motors while collecting gravel.

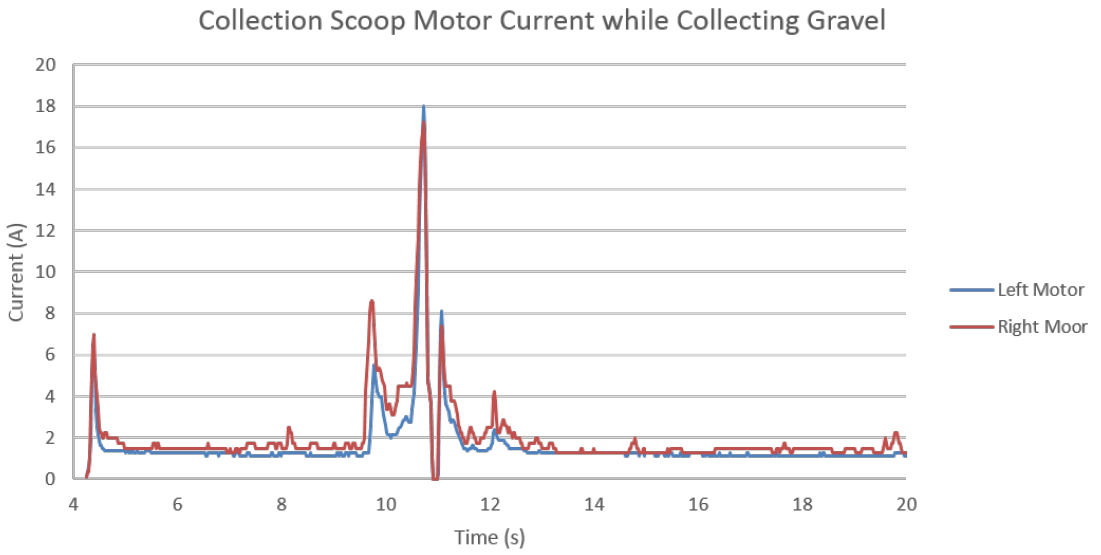

Figure 65: Current in the left and right scoop motors while collecting gravel

As expected, the idle current in both of the motors remained about the same at 1.5 A, but the current required to actually scoop the gravel was significantly higher. The left and right motors peaked at 18 A and 17.25 A, respectively. Because gravel is less fluid than sand, it requires more force to penetrate between the rocks, which in turn yields a much higher current produced by the motors. Assuming a worst case current draw of 35.25 A, the collection system would use 423 W. Assuming the robot spends 3 minutes collecting gravel, this worst case scenario would use 1.18 Ah (6.56% of the battery's capacity).

5.4 Material Deposit Evaluation

In order to test the capabilities of the mining platform's material deposit system, the bucket was retracted as far as possible. It was then filled with varying amounts of sand to determine the point at which it was no longer capable of dumping material. The robot successfully dumped 100 kg of material as per the design specifications, but failed to remove a 110 kg load. Fortunately, the bucket was filled to nearly overflowing with material when 110 kg was added, so the possibility of reaching a point when the bucket can no longer remove its load is minimal.

Figure 66: Lifting and depositing material

6 Future Work

The mining platform was designed to operate in a Martian environment in part to compete in NASA's Robotic Mining Challenge. This meant that the rover only needed to operate over a ten minute period, and many of the rover components would not necessarily last during a long term mission on Mars. In addition to making the mining platform better outfitted for a Mars mission, several other improvements have been outlined below. These improvements would increase the overall robustness and stability of the system.

6.1 Increased Gearbox Structural Support

While the synchronized dump sequence worked relatively well, the large forces involved with the operation led to structural concerns in the gearbox and output shaft for the mechanism. The forces on the shaft which drove the winch and four bar linkage were so large that the shaft would bend; this increased the overall friction in the gearbox and caused the CIM motors to use significantly more current to actuate the mechanism. While adding more structural support to the gearbox would solve the problem, the easiest solution would be to upgrade the 1/2 in aluminum hex shaft to a larger diameter shaft, or switch it to a steel keyed shaft to limit flex in the system.

6.2 Improved Autonomy

Augmented autonomy was implemented on the robotic mining platform for its three major operations of driving, digging and dumping. However, for this project, manual control via human intervention was expected. Through the addition of more sensors and a more rigorous sensing algorithm, full autonomy could be achieved. One of the major challenges in designing a fully autonomous system is dealing with inaccuracies in the feedback from the on-board sensors. For example, while a drive encoder may correctly report how much the sprocket has spun, it will not provide any feedback to determine if the belt is free spinning or slipping in the regolith. In order to remedy this, feedback from multiple sensors should be combined through a Kalman filter; for example, by using the camera for measuring velocity, it would be possible to determine if the robot was stuck, as the camera would not report any movement with relation to the markers.

6.3 More Accurate Material Collection Estimates

The IR sensors used provided a reasonable estimate of the material collected, but have a few weaknesses. Dust produced by dumping material in the bucket would temporarily obstruct the IR sensors, causing their readings to become temporarily inaccurate. Furthermore, the geometry of the sand in the bucket has an effect on the readings of the IR sensors; depending on the positioning of the IR sensors, a peak of sand in the center of the bucket could lead to reporting that the entire bucket is actually full. The better solution to estimating the weight of material in the bucket would be to add several strain gauges to the bottom of the bucket. Because the deflection of the strain gauge should correlate linearly to the mass of material collected, this would provide a much more accurate estimate of the material collected. This also removes the issue of the weight estimate being dependent on how the material is distributed throughout the bucket.

6.4 Increased Dust Resilience

The scoop ladder collection system is powered by a 3/8 in pitch chain system. This chain often gets coated with regolith during operation which can damage the chain after extended use. During long term operation the chain would be very likely to break or fall off the sprockets; this would never happen during the 10 minute operational period that the robot was designed for. However, for implementation on an actual Mars mission, a belt system should be implemented along with custom attachments for scoops. Unlike chains, belts do not require oil or grease, are less prone to deformation, and are comprised of a single object instead of multiple smaller links. A belt system would also decrease the overall weight of the system.

6.5 Higher Chassis Clearance

The mining platform was designed to be able to traverse a Martian environment populated with craters and rocks. While the current system is able to do this, it sometimes gets stuck in craters that are greater than a foot deep. In this case, the robot battery and winch/four bar gearbox become caught in the regolith, causing the robot to become motionless. For future iterations of this project, these features should be raised up higher off the ground to prevent this issue. The physical size of the battery should also be considered, as the extent to which the battery can be raised up is limited by its size.

7 Conclusion

The material presented in this report describes the course of actions taken since August 2016 to transform the robot from an idea into reality. The robot's three subsystems were carefully designed to ensure the robot would be capable of collecting a significant amount of regolith and ice. At the time of writing this paper, the team is still in the process of finalizing parts of the robot in order to prepare it for the 2017 NASA Robotics Mining Competition. Table 3 shows the goals originally set by the team and the specifications the robot is expected to have at the end of its construction.

Parameter	Specification	Requirement Met
Maximum Size	1.5 m × 0.75 m × 0.75 m	Met (1.02 m × 0.71 m × 0.74 m)
Maximum Weight	80 kg	Met (80 kg)
Battery life	10 minutes	Met (20 minutes)
Payload Capacity	Capable of transporting at least 50 kg of combined BP-1 and gravel in a single payload.	Met (100 kg)
Material Collection	Capable of collecting at least 10 0kg of combined BP-1 and gravel within a 10-minute time frame.	In Progress
Gravel Collection	Capable of collecting at least 20 kg of gravel within a 10-minute time frame.	In Progress
Control	Capable of executing autonomous subroutines (such as driving to a specific location or collecting a full payload).	Met

Table 3: Met requirements

With the exception of "Material Collection" and "Gravel Collection", all of these requirements have been met. At the time of submission, the remaining robot scoops were in the process of being manufactured and would have been required to

accurately determine if the appropriate amounts of material could be collected in the specified time frame. Based on testing with a single scoop, it is expected that the robot will meet these requirements.

Appendix A: Mining Calculations

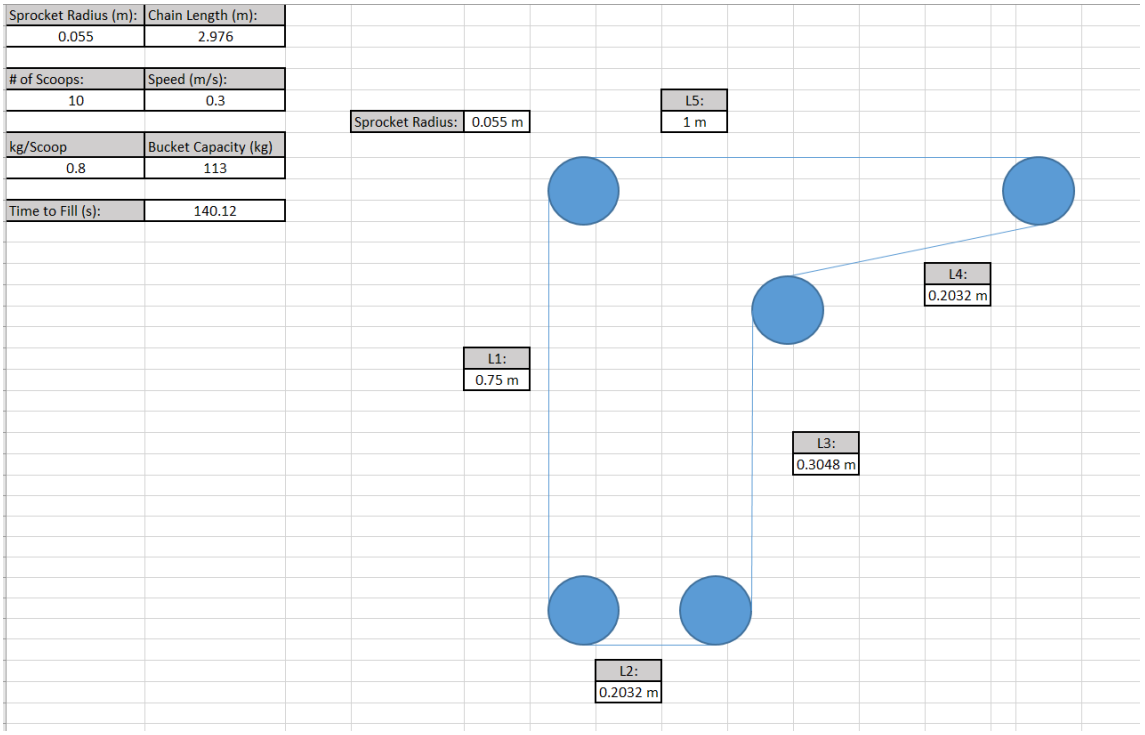

Figure 67: Calculated rate of gravel and regolith collection

Collection System Analysis

Vexpro 775 Motor Constants

$MaxPower_{775} := 347W \quad StallTorque_{775} := .71N \cdot m \quad FreeCurrent_{775} := 0.7A \quad FreeSpeed_{775} := 18730rpm$

Excavation Power Transmission

Known constants from experimentation with drill & design

$OutputSpeed_{collector} := 0.25\frac{m}{s} \quad ExcavationTorque_{measured} := 16.95N \cdot m \quad SafetyFactor_{Collection} := 2$

$CollectorSprocket_{diameter} := 0.0851in \quad Time_{excavating} := 300s \quad CollectionRPM := 56.1rpm$

Calculations for gearbox required on VexPro 775 motor:

$Torque_{excavation} := SafetyFactor_{Collection} \cdot ExcavationTorque_{measured} = 33.9\,N \cdot m$

$Force_{excavation} := \frac{Torque_{excavation}}{CollectorSprocket_{diameter}} = 1.568 \times 10^{4} \cdot N$

$TorqueRequired_{775} := Torque_{excavation} = 33.9 \cdot N \cdot m$

Pick an available gearbox to give us our diesired output speed at an optimal point on the motor curve

$OptimalMotorSpeed_{775} := 15000rpm \quad OptimalTorque_{775} := 0.4N \cdot m$ From motor curve

$GearboxRequired_{775} := \frac{OptimalMotorSpeed_{775}}{CollectionRPM} = 267.38 \quad GearBox_{775} := 256$ Select gearbox of 256

Verify that this gearbox satisfies our desired torque requirment with our factor of safety

$Scoop_{torque} := OptimalTorque_{775} \cdot GearBox_{775} = 102.4 \cdot N \cdot m$ Output torque is sufficient

Figure 68: Validation of 775pro motor paired with 256:1 gearbox

											Efficiency	Input Torque(Nm)	Output Torque(Nm)	Input RPM	Output RPM	Output Speed(in/s)	Gear Ratio
Mass	80.00	kg		Actual Output Torque	24.41	Nm		Max Input Torque	4.07	Nm	0.00	0.00	0.00	104.00	#DIV/0!	#DIV/0!	0.00
Ouput Speed	1.50	in/s		Output RPM	13.83			Input RPM	83.00		47.57	1.36	25.76	97.07	5.11	0.68	19.00
Output Sprocket Radius	1.27	in									55.72	2.71	27.12	90.13	9.01	1.20	10.00
Max Output Torque	25.51	Nm									56.34	4.07	28.48	83.20	11.89	1.58	7.00
				Ratio	6.00						54.23	5.42	27.12	76.27	15.25	2.03	5.00
											50.83	6.78	27.12	69.33	17.33	2.31	4.00
	1.45										46.71	8.14	32.54	62.40	15.60	2.08	4.00
											42.16	9.49	28.48	55.47	18.49	2.46	3.00
											37.31	10.85	32.54	48.53	16.18	2.15	3.00
											32.28	12.20	36.61	41.60	13.87	1.85	3.00
											27.09	13.56	27.12	34.67	17.33	2.31	2.00
Diameter for Sprocket	2.54										21.81	14.92	29.83	27.73	13.87	1.85	2.00
											16.44	16.27	32.54	20.80	10.40	1.38	2.00
											11.01	17.63	35.26	13.87	6.93	0.92	2.00
											5.52	18.98	37.97	6.93	3.47	0.46	2.00
											0.00	20.34	40.68	0.00	0.00	0.00	2.00

Figure 69: Torque Calculations to determine gear ratio for carriage actuator

Appendix B: Budget and Spending

Category	Compents	Cost
Mechanical		
	Brecoflex	1500
	Chain Actuation Compenents (sprockets, bearings, axles)	1250
	Robot Base Stock for Manufacturing	1000
	Misc Hardware	500
	Scoops	1000
Electrical		
	Motors & Motor Controllers	1000
	Battery	200
	Sensors	300
	Boards	250

Figure 70: Planned Budget

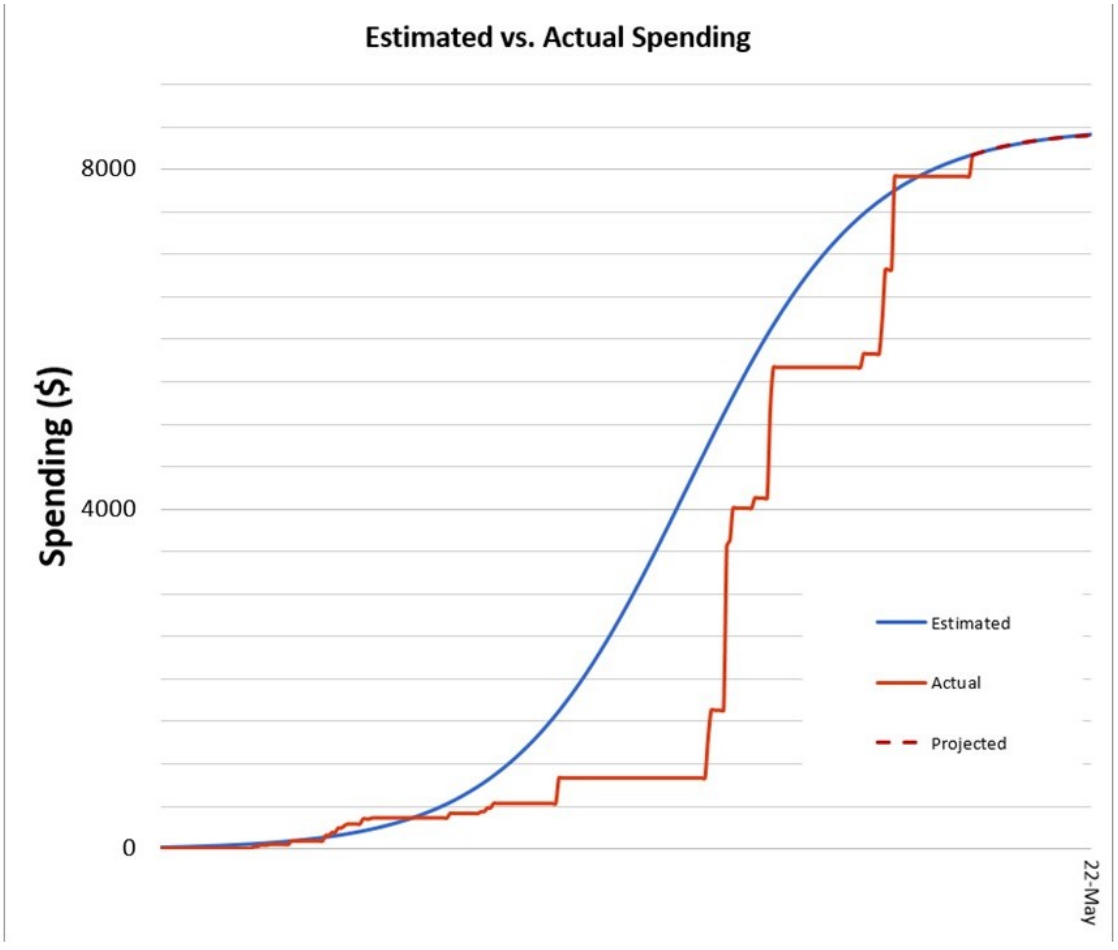

Figure 71: Spending curve: Expected Vs. Reality

Appendix C: Prototype Rigs

Figure 72: First digging rig

Figure 73: Second digging rig

Figure 74: Driving Pit

Figure 75: Robot Digging Test Rig

Appendix D: Manufacturing

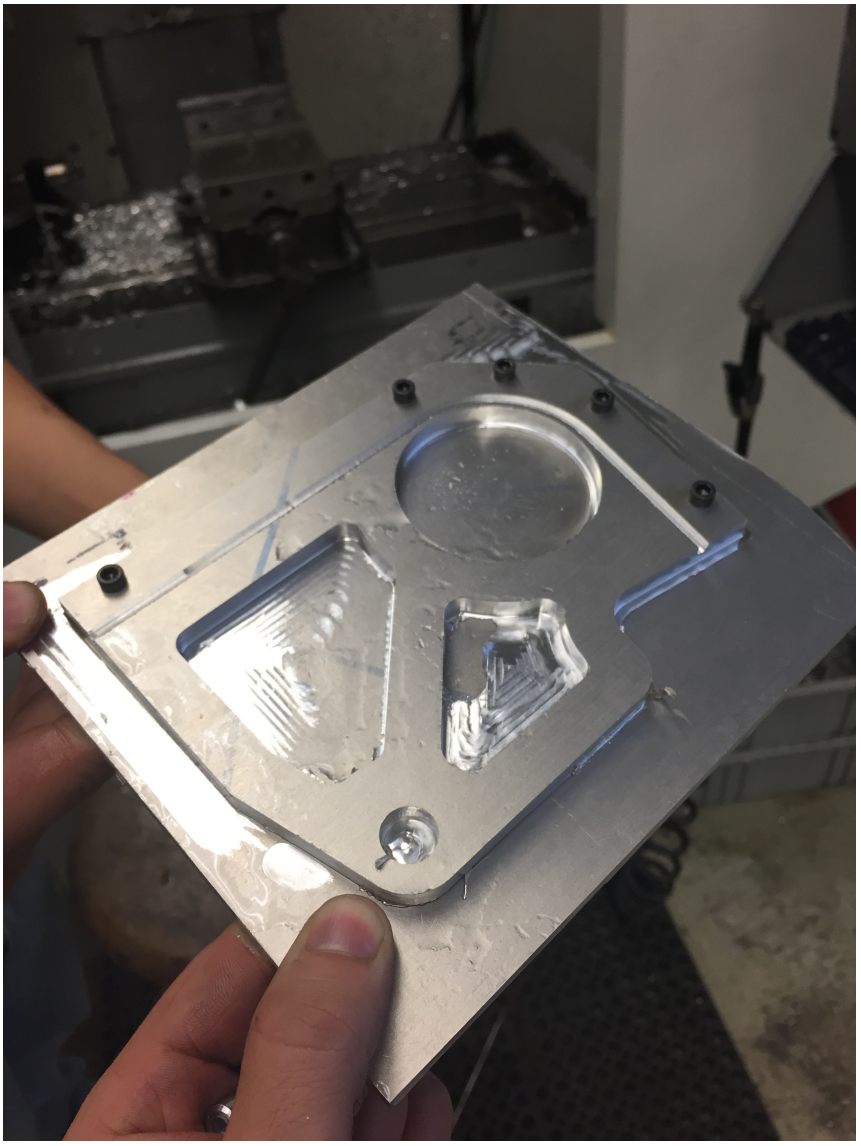

Figure 76: Guide for Regulator Tape

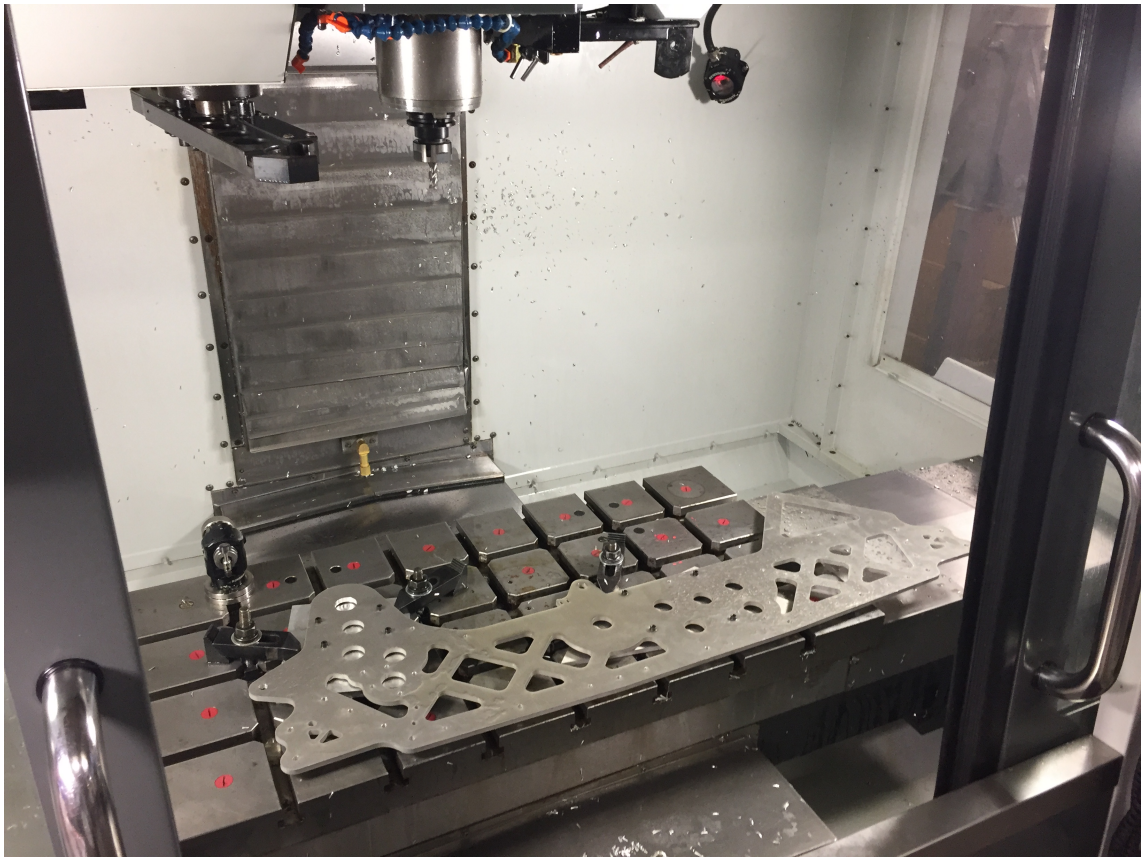

Figure 77: Inside drive plate fixtured to bore bearing holes

Figure 78: Axles for custom sprockets

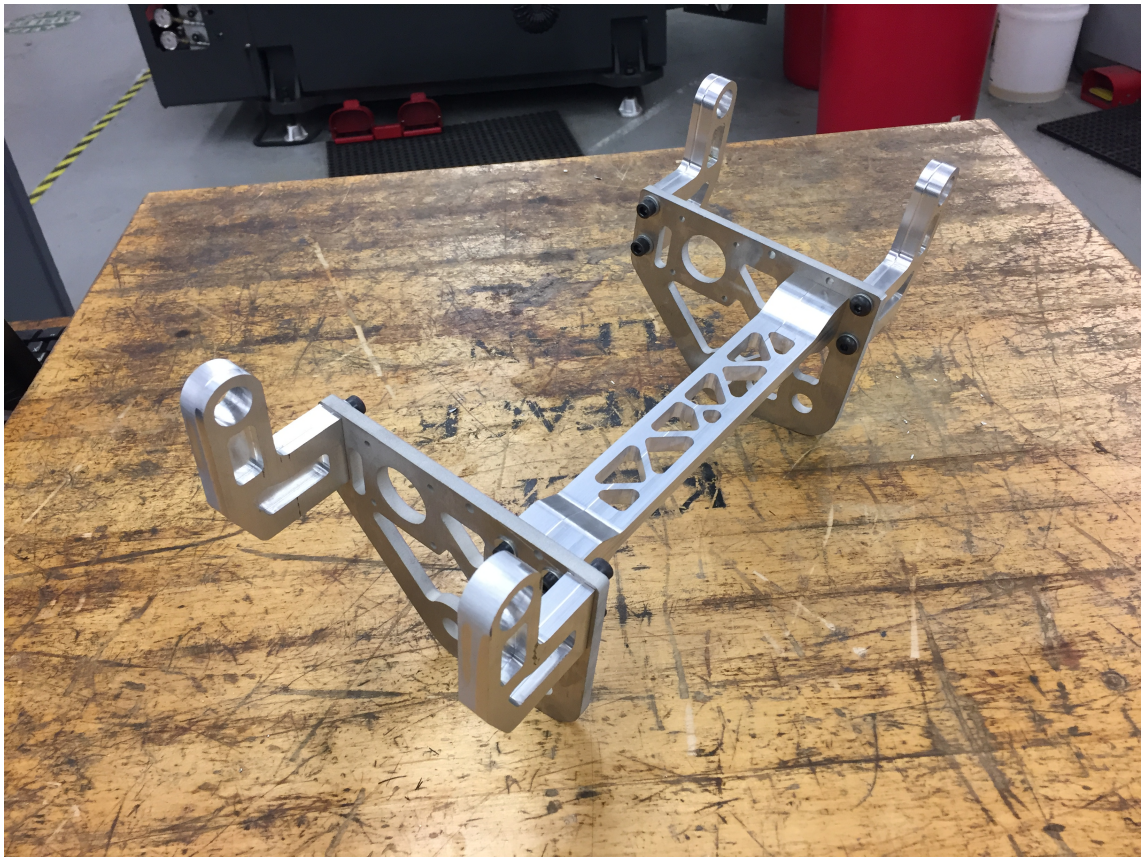

Figure 79: Upper Carriage

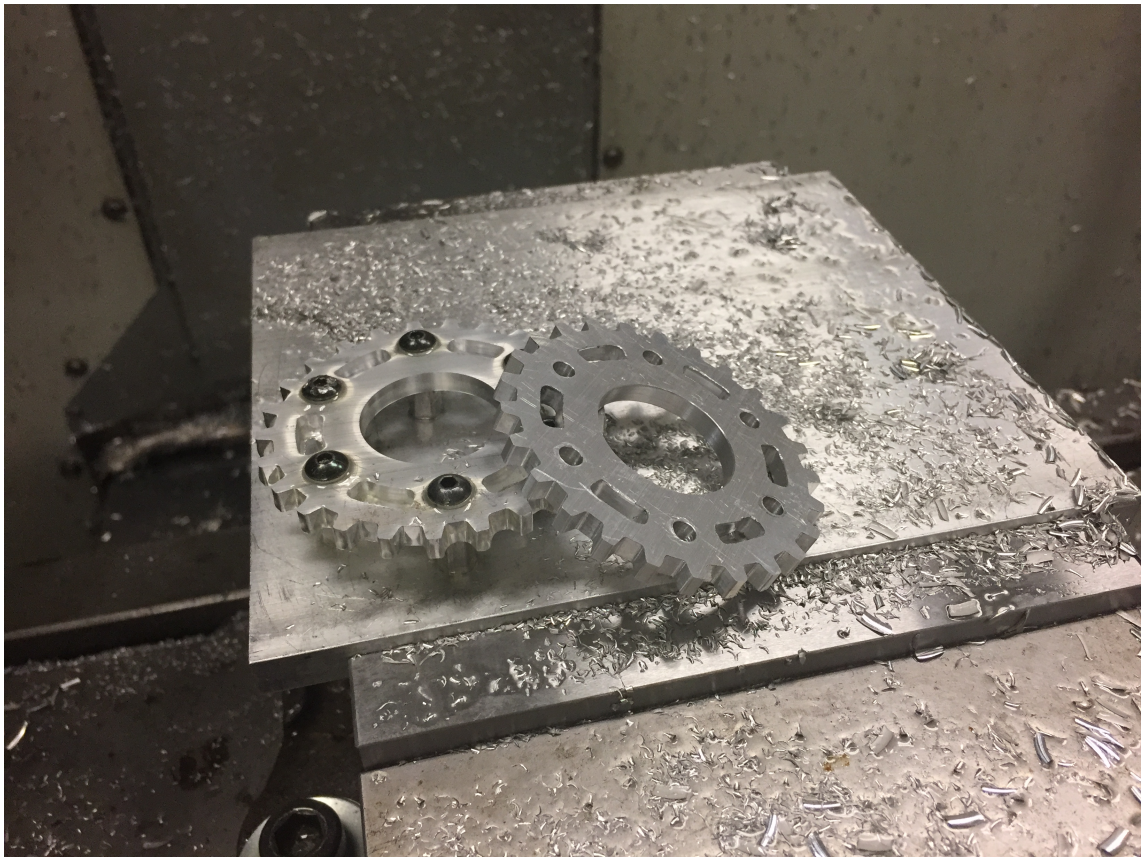

Figure 80: Sprockets for Regulator Tape

Figure 81: Custom Idler Sprockets

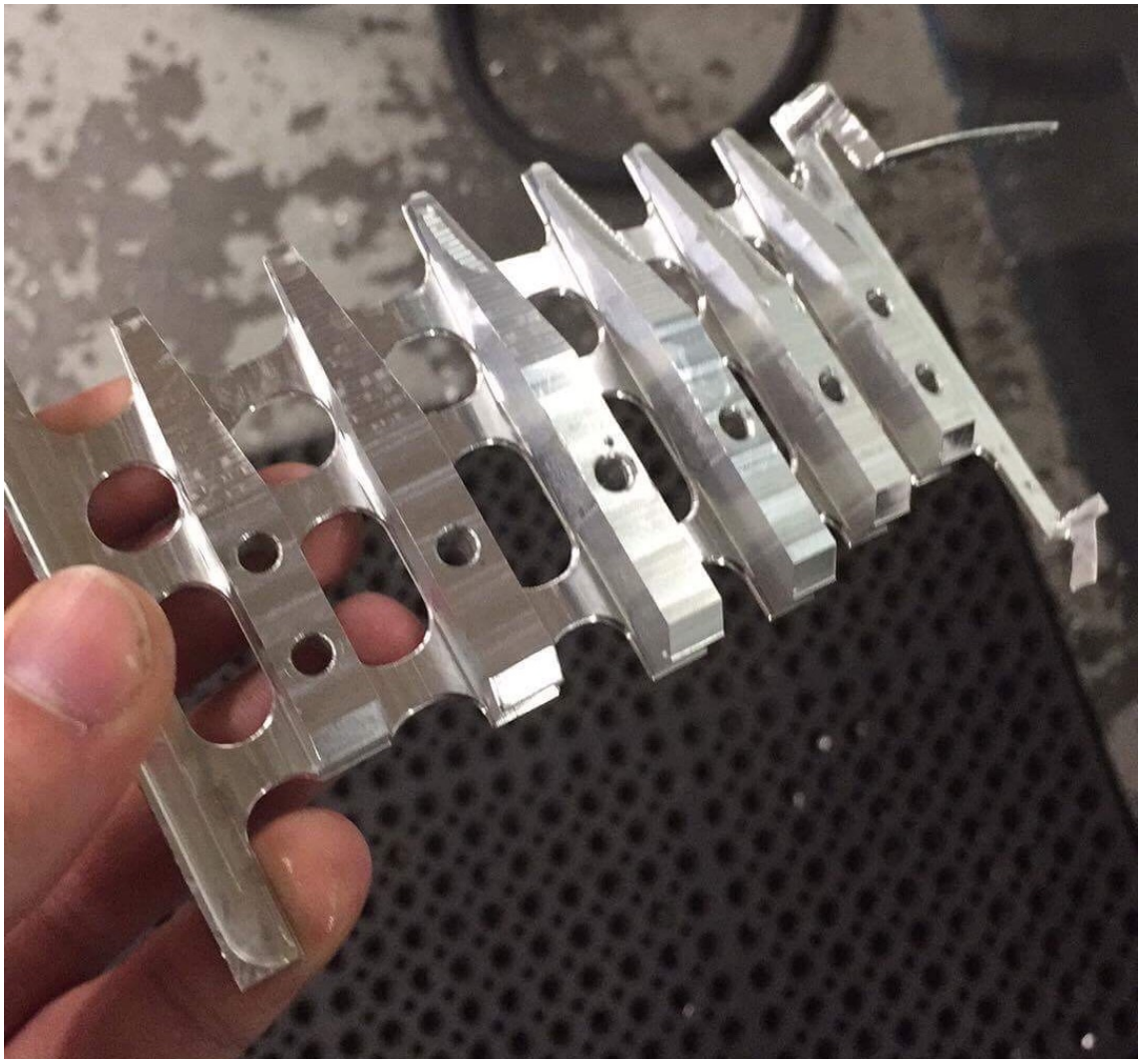

Figure 82: Scoop teeth manufactured from single plate